

# 1 Surface and sub-surface multi-proxy reconstruction of 2 middle to late Holocene palaeoceanographic changes in 3 Disko Bugt, West Greenland

4 Matthias Moros<sup>1\*</sup>, Jeremy M. Lloyd<sup>2</sup>, Kerstin Perner<sup>1</sup>, Diana Krawczyk<sup>3</sup>, Thomas Blanz<sup>4</sup>, Anne de  
5 Vernal<sup>5</sup>, Marie-Michele Ouellet-Bernier<sup>5</sup>, Antoon Kuijpers<sup>6</sup>, Anne E. Jennings<sup>7</sup>, Andrzej Witkowski<sup>8</sup>,  
6 Ralph Schneider<sup>4</sup>, Eystein Jansen<sup>9,10</sup>

7  
8 1 Leibniz Institute for Baltic Sea Research, Department of Marine Geology, Germany

9 2 Durham University, Department of Geography, UK

10 3 Greenland Climate Research Centre, Greenland Institute of Natural Resources, Greenland

11 4 Institute of Geosciences, Department of Geology, Kiel University, Germany

12 5 GEOTOP, Université du Québec à Montréal, Canada

13 6 Geological Survey of Denmark and Greenland, Copenhagen, Denmark

14 7 Institute of Arctic and Alpine Research, University of Colorado, United States

15 8 Faculty of Geosciences, University of Szczecin, Mickiewicza 18, 70-383 Szczecin, Poland

16 9 Bjerknes Centre for Climate Research, Allégaten 55, Bergen 5007, Norway

17 10 Department of Earth Science, University of Bergen, and Bjerknes Centre for Climate Research, Allégaten 70,  
18 Bergen 5007, Norway

19  
20 \*Corresponding author: Matthias Moros

21 Leibniz Institute for Baltic Sea Research

22 See Str. 15, 18119 Rostock, Germany

23 E-mail: [matthias.moros@io-warnemuende.de](mailto:matthias.moros@io-warnemuende.de)

24 Tel.: +49/381/5197399

25  
26 Keywords: Sea surface temperature, alkenone %C<sub>37:4</sub>, diatoms, benthic foraminifera,  
27 dinocysts, West Greenland Current, Disko Bugt, Holocene

## 28 29 Abstract

30 We present new surface water proxy records of meltwater production  
31 (alkenone derived), relative sea surface temperature (diatom, alkenones) and sea  
32 ice (diatoms) changes from the Disko Bugt area off central West Greenland. We  
33 combine these new surface water reconstructions with published proxy records  
34 (benthic foraminifera - bottom water proxy; dinocyst assemblages – surface water  
35 proxy), along with atmospheric temperature from Greenland ice core and Greenland  
36 lake records. This multi-proxy approach allows us to reconstruct centennial scale  
37 middle to late Holocene palaeoenvironmental evolution of Disko Bugt and the  
38 Western Greenland coastal region with more detail than previously available.

39 Combining surface and bottom water proxies identifies the coupling between  
40 ocean circulation (West Greenland Current conditions), the atmosphere and the  
41 Greenland Ice Sheet. Centennial to millennial scale changes in the wider North  
42 Atlantic region were accompanied by variations in the West Greenland Current  
43 (WGC). During periods of relatively warm WGC, increased surface air temperature  
44 over western Greenland led to ice sheet retreat and significant meltwater flux. In

45 contrast, during periods of cold WGC, atmospheric cooling resulted in glacier  
46 advances.

47 We also identify potential linkages between the palaeoceanography of the  
48 Disko Bugt region and key changes in the history of human occupation. Cooler  
49 oceanographic conditions at 3.5 ka BP support the view that the Saqqaq culture left  
50 Disko Bugt due to deteriorating climatic conditions. The cause of the disappearance  
51 of the Dorset culture is unclear, but the new data presented here indicate that it may  
52 be linked to a significant increase in meltwater flux, which caused cold and unstable  
53 coastal conditions at ca. 2 ka BP. The subsequent settlement of the Norse occurred  
54 at the same time as climatic amelioration during the Medieval Climate Anomaly and  
55 their disappearance may be related to harsher conditions at the beginning of the  
56 Little Ice Age.

57

58

## 59 **1. Introduction**

60 From the perspective of future climate change, the behaviour of the  
61 Greenland Ice Sheet (GIS) is of critical interest, due to its potential impact on global  
62 sea-level changes and ocean circulation (e.g. Howat et al., 2007; Pritchard et al.,  
63 2009). Enhanced freshwater contribution of the GIS to the North Atlantic Ocean may  
64 affect the northward heat transport in the North Atlantic Drift (Oppo et al., 2003;  
65 Thornalley et al., 2009, Moros et al., 2012). Many tidewater glaciers in southeast and  
66 west Greenland show significant changes in velocity and consequent ice flux to the  
67 ocean since 2000 (e.g. Andresen et al., 2013; Holland et al., 2008; Howat et al.,  
68 2007, 2008, 2011; Moon and Joughin, 2008; Rignot and Kanagaratnam, 2006;  
69 Straneo et al., 2010; Walsh et al., 2012; Zwally et al., 2002). The forcing  
70 mechanism for the enhanced ice velocity is unclear although there is strong support  
71 for the importance of the influence of changing ocean temperatures driving glacier  
72 dynamics (e.g. Holland et al., 2008; Lloyd et al., 2011; Rignot et al., 2010). On longer  
73 time scales the 'ocean forcing' may have played an important role in triggering large-  
74 scale ice sheet destabilization (e.g. Moros et al., 2002). A better understanding of the  
75 linkages between past GIS behaviour and forcing mechanisms such as changes in  
76 ocean circulation is, therefore, critical to predicting future changes in ice sheet  
77 behaviour.

78 The area of Disko Bugt in central west Greenland has been of particular  
79 interest because of the significant changes in ice velocity of Jakobshavn Isbræ, one  
80 of the largest ice streams draining approximately 7% of the GIS (Bindschadler,  
81 1984). This area has been intensively studied over recent years with special  
82 attention paid to the late Quaternary variation of the ice sheet (e.g. Briner et al.,  
83 2010; Kelley et al., 2013; Larsen et al., 2015; Weidick and Bennike, 2007; Young et  
84 al., 2011), the deglaciation and the Holocene variations in nearshore to offshore  
85 ocean circulation (e.g. Lloyd et al., 2005, 2007, 2011; Jennings et al., 2014;  
86 Krawczyk et al., 2010, 2012, 2013; Moros et al., 2006b; Ouellet-Bernier et al., 2014;

87 Perner et al., 2011, 2013a,b; Ribeiro et al., 2012; Seidenkrantz et al., 2008). More  
88 recently, a number of studies from Disko Bugt have identified areas of high  
89 accumulation rate, suitable for investigating decadal to multi-centennial scale  
90 variations in ocean circulation (site 343310 and 343300, Figure 1; Lloyd et al., 2011;  
91 Perner et al., 2011, 2013a). To date, the studies from Disko Bugt have focused on a  
92 limited number of proxies, commonly either surface water proxies (diatoms,  
93 dinocysts; e.g. Krawczyk et al., 2010, 2013; Ribeiro et al., 2012; Ouellet-Bernier et  
94 al., 2014) or bottom water proxies (benthic foraminifera; e.g. Lloyd et al., 2005, 2007,  
95 2011; Perner et al., 2011, 2013a).

96 Here, we combine published surface (diatoms, dinocysts) and sub-surface  
97 (benthic foraminifera) water proxy data (343310: Krawczyk et al., 2013; 343300:  
98 Ouellet-Bernier et al., 2014; 343310: Lloyd et al. 2011; Perner et al., 2011; 343300:  
99 Perner et al., 2013a) from these core sites (Figure 1) with new records of sea  
100 surface salinity (the relative proportion of tetra-unsaturated  $C_{37}$  ketones -  $\%C_{37:4}$  - in  
101 alkenones) and relative estimates of sea surface temperature (biomarker alkenone  
102 derived  $U_{37}^k$ , diatoms in 343300). By combining the different proxies (measured on  
103 the same sample sets) and by comparing our marine data with terrestrial lake and  
104 the ice core records, a more complete picture of the evolution of ocean circulation,  
105 atmospheric temperature and ice stream behaviour over the middle to late Holocene  
106 can be proposed. Linkages between climate and the history of human occupation of  
107 West Greenland, along with middle to late Holocene ocean circulation changes  
108 observed off West Greenland in the broader context of the North Atlantic are also  
109 discussed.

110

## 111 **2. Study area and regional environmental setting**

112 Disko Bugt (Figure 1) is a large marine embayment (40,000 km<sup>2</sup>) off central  
113 West Greenland with relatively shallow water depths of 200 to 400 m and with  
114 maximum water depths up to 900 m in Egedesminde Dyb, a deep-water trough of  
115 glacial origin (Long and Roberts, 2003; Roberts and Long, 2005; Zarudski, 1980).  
116 The Disko Bugt area is typically covered by seasonal sea-ice from January to March-  
117 April/May and the present day climatic conditions are low arctic maritime with mean  
118 surface air temperatures of  $\sim 4.8^{\circ}\text{C}$  in summer and  $\sim -5.2^{\circ}\text{C}$  throughout the year  
119 (Fredskild, 1996, Nielsen et al., 2001; Ribergaard et al., 2006).

120 The West Greenland Current (WGC), which dominates the regional  
121 oceanography is a water mass resulting from the mixing of: (i) Arctic-sourced cold,  
122 low-salinity water from the East Greenland Current (EGC, found at 0-200 m water  
123 depth), termed Polar Water (Buch, 1981); (ii) relatively warm and saline Atlantic-  
124 sourced water from the Irminger Current (IC, >200 m water depth), a branch of the  
125 North Atlantic Current (NAC; Buch, 1981; Tang et al., 2004); and (iii) surface local  
126 meltwater discharge from the south-west Greenland margin. The WGC is formed at  
127 the southern tip of Greenland (Cape Farwell) and flows northwards on the West  
128 Greenland shelf (Cuny et al., 2002) and turns gradually westwards into Baffin Bay.

129 Reaching central West Greenland, a side branch of the WGC enters Disko Bugt from  
130 the southwest and flows northwards exiting the embayment primarily through the  
131 Vaigat Strait (Figure 1 and inset; Andersen, 1981; Bâcle et al., 2002; Ribergaard et  
132 al., 2006). Along its flow path in Disko Bugt, the WGC carries icebergs and meltwater  
133 from outlet glaciers located in eastern Disko Bugt, such as Jakobshavn Isbræ,  
134 Semerq Avangnardleq, Sermeq Kujadleq and Kangersuneq (Figure 1). Exiting Disko  
135 Bugt through the Vaigat Strait, a branch of the WGC deflects westwards into Baffin  
136 Bay, while the major current continues to flow further northwards along the West  
137 Greenland coast. The Atlantic Water core of the WGC is relatively warm and saline  
138 with temperatures  $> 5^{\circ}\text{C}$  and salinity  $> 34.9$  PSU off Cape Farewell gradually cooling  
139 and freshening to  $3.5\text{-}4.5^{\circ}\text{C}$  and  $34.2\text{-}34.9$  PSU in the Disko Bugt area forming the  
140 bottom waters in Disko Bugt and the adjacent shelf (Andersen, 1981; Buch, 1981;  
141 Buch et al., 2004; Lloyd, 2006; Ribergaard et al., 2013). There are no indications that  
142 deep Baffin Bay waters penetrate onto the shelf along the west Greenland margin or  
143 into Disko Bugt below 300 m water depth (Andersen, 1981). However, meltwater flux  
144 and icebergs from outlet glaciers, as well as the winter season's pack ice and low-  
145 salinity polar surface water from Baffin Bay influence surface water properties along  
146 the west Greenland margin. In the Disko Bugt area, sea-surface conditions record  
147 large variations. Sea-surface conditions at coring site 343300 (Figure 1) show  
148 significant interannual variability: data compiled from the National Oceanographic  
149 Data Center (NODC, 2001) indicate mean summer sea-surface temperature of  $3.1$  to  
150  $5.7^{\circ}\text{C}$  (one sigma) and salinity of  $32.9$  to  $33.4$ ; 1953-2003 data from the National  
151 Snow and Ice Data Center (NSIDC) indicate mean sea-ice cover of  $3.8 \pm 1.3$   
152 months/yr. Surface water productivity in Disko Bugt is influenced by the nearby sea  
153 ice edge of the so-called 'West Ice', which forms in Baffin Bay during late autumn  
154 and winter. At present this frontal zone lies northwest of Disko Bugt in spring  
155 (Hansen et al., 1999; Levinsen et al., 2000; Tang et al., 2004).

156

### 157 **3. Methods**

#### 158 **3.1 Chronology**

159 The age control of cores 343300 and 343310 (Figure 1) is provided by  
160 accelerator mass spectrometry (AMS)  $^{14}\text{C}$  dates on benthic foraminifera and mollusc  
161 shells, calibrated with Marine09 (Reimer et al., 2009) using OxCal 4.1 (Bronk  
162 Ramsey, 2009) and a marine reservoir age correction  $\Delta R$  of  $140 \pm 35$  years (Lloyd et  
163 al., 2011). For full details of core chronologies see Perner et al. (2011, 2013a). Multi  
164 core (MUC) and gravity core (GC) records from both core sites do not overlap. At  
165 site 343300 there is a 500 year gap between MUC and GC and at site 343310 there  
166 is a gap of ca. 100 years between MUC and GC. The chronology of core 343310 is  
167 based on a larger number of AMS  $^{14}\text{C}$  dates and the core is characterized by a higher  
168 sedimentation rate than core 343300. Therefore, discussions on the timing of late  
169 Holocene oceanographic changes are based on core 343310.

170

## 171 **3.2 Multi-proxy approach**

172 The combination of proxies presented here provides information on a range of  
173 oceanographic parameters. The individual studies were performed on samples from  
174 the same depths except where resolution differed between proxies. The alkenone  
175 biomarker derived data ( $\%C_{37:4}$ ,  $U_{37}^k$ ) provide information on salinity variations and  
176 relative sea-surface temperature (SST); diatom and dinocyst assemblages provide  
177 estimates of sea surface temperature, salinity and sea ice conditions, which are used  
178 qualitatively here; benthic foraminifera provide information on bottom conditions, in  
179 particular the relative strength of the Atlantic water component of the WGC, but also  
180 on supply of organic material linked to surface water productivity.

181

### 182 **3.2.1 Alkenone biomarkers**

183 *Analytical method:* Alkenones are specific organic compounds synthesized by  
184 haptophyte algae such as coccolithophores. In this study alkenone ( $U_{37}^k$ ,  $\%C_{37:4}$ )  
185 analyses were carried out at the Biomarker Laboratory of the University of Kiel. At  
186 site 343300, samples were analyzed every 3 cm with a temporal resolution of about  
187 70 years, covering the time period from ca. 8 ka BP and at site 343310 every 4 cm  
188 with a temporal resolution of 12-15 years for the time period from ca. 3.6 ka BP.  
189 Long-chained alkenones ( $C_{37}$ ) were extracted from homogenized bulk sediment (2 to  
190 3 g), using an Accelerated Solvent Extractor (Dionex ASE-200) with a mixture of 9:1  
191 (v/v) of dichloromethane:methanol (DCM:MeOH) at 100°C and 100 bar  $N_2$  (g)  
192 pressure for 20 minutes. At c. -20°C extracts were cooled and subsequently taken to  
193 near dryness by Synore polyvap at 40°C and 490 mbar. We used a multi-  
194 dimensional, double gas column chromatography (MD-GC) set up with two Agilent  
195 6890 gas chromatographs for  $C_{37:2}$ ,  $C_{37:3}$  and  $C_{37:4}$ , identification and quantification  
196 (Etourneau et al., 2010). Quantification of the organic compounds was achieved with  
197 the addition of an internal standard prior to extraction (cholestane [ $C_{27}H_{48}$ ] and  
198 hexatriacontane [ $C_{36}H_{74}$ ]). The proportion of each alkenone was obtained using the  
199 peak areas of the specific compounds. The  $U_{37}^k$  index is calculated using the  
200 equation from Prahl et al. (1987):  $U_{37}^k = (C_{37:2}) / (C_{37:2} + C_{37:3})$ ,  $U_{37}^k$  index according to  
201 Brassell et al. (1986):  $U_{37}^k = (C_{37:2} - C_{37:4}) / (C_{37:2} + C_{37:3} + C_{37:4})$ . However, Rosell-Melé  
202 (1998) and Bendle and Rosell-Melé (2004) point out that  $U_{37}^k$  based estimates are  
203 more robust down to 6°C than  $U_{37}^{k'}$ .

204 *Proxy for sea surface temperature:* We present a high-resolution record of the  
205 alkenone unsaturation index  $U_{37}^k$  to reconstruct relative SST changes for the middle  
206 to late Holocene. However, as noted earlier (Rosell-Melé, 1998) at  $C_{37:4}$  values  
207 above 5 % – which is the case here – alkenone based SSTs have increasing errors.  
208 Therefore we use the alkenone-based temperature reconstructions qualitatively  
209 (using the  $U_{37}^k$ ) rather than quantitatively here.

210  $\%C_{37:4}$  – *Proxy for meltwater input:* We also present the proportion of tetra-  
211 unsaturated  $C_{37}$  ketones relative to the sum of alkenones ( $\%C_{37:4}$ ) for the middle to  
212 late Holocene. This ratio serves as an indicator of changes in meltwater discharge  
213 from the GIS as the amount of  $C_{37:4}$  rises at lower surface salinities in polar and sub-

214 polar waters (Rosell-Melé, 1998; Rosell-Melé et al., 2002; Sicre et al., 2002; Harada  
215 et al., 2003; Bendle et al., 2005; Blanz et al., 2005).

216

### 217 **3.2.2 Diatom analyses**

218 *Preparation and counting method:* Diatom counting results of site 343310 are  
219 published in Krawczyk et al. (2013), and gravity core results of site 343300 are  
220 presented here for the first time. The 343300 samples were prepared using a  
221 chemical cleaning process (hydrochloric acid and hydrogen peroxide) and  
222 microscope slides were prepared following the method described in Krawczyk et al.  
223 (2013). The identification of species was carried out using light microscopy and  
224 scanning electron microscopy. For each sample over 300 valves were counted,  
225 excluding unidentifiable *Chaetoceros* resting spores (after Schrader and Gersonde,  
226 1978). Identification of diatom species follows Fryxell (1975), Syvertsen (1979),  
227 Hasle and Syvertsen (1996), Witkowski et al. (2000), Quillfeldt (2001), Throndsen et  
228 al. (2003).

229 *Ecological preferences:* In arctic environments the diatom flora can be used to  
230 investigate surface water characteristics based on the ecological preferences of key  
231 indicator species (e.g. Koç Karpuz and Schrader, 1990; Justwan and Koç, 2008;  
232 Krawczyk et al., 2012, 2014). Two selected key species, *Fragilariopsis cylindrus* and  
233 *Thalassiosira kushirensis* resting spores (r.s.), are used here based on their specific  
234 ecological preferences associated with surface water characteristics (Hasle and  
235 Syvertsen, 1996; Krawczyk et al., 2014). *Fragilariopsis cylindrus* is associated with  
236 sea-ice (e.g. Koç Karpuz and Schrader, 1990; Jiang et al., 2001; Justwan and Koc,  
237 2008) and cold, open marine waters, and occurs mainly in arctic regions (Quillfeldt,  
238 2001, 2004). This species is abundant in Disko Bugt in spring-summer (Jensen,  
239 2003), suggesting that meltwater is important for blooms of this species (Krawczyk et  
240 al., 2013). Krawczyk et al. (2014) observed *Fragilariopsis cylindrus* in modern water  
241 samples mainly in the northern-most samples of the West Greenland coastal waters,  
242 associated with sea ice and/or strong meltwater flux. *Thalassiosira kushirensis* r.s. is  
243 known to have a sub-Arctic and Arctic distribution (Hasle and Syvertsen, 1996;  
244 Krawczyk et al., 2012; Weckström et al., 2014), and in previous studies from Disko  
245 Bugt this species has been linked to temperate waters (Krawczyk et al., 2010, 2013).  
246 It should be noted that in different regions of the North Atlantic three morphologically  
247 similar species have been identified: *Thalassiosira kushirensis* r.s. (e.g. Krawczyk et  
248 al., 2013); *Thalassiosira antarctica* var. *borealis* r.s. (e.g. Jiang et al., 2001) and;  
249 *Thalassiosira gravida* r.s. (e.g. Koç Karpuz and Schrader, 1990), each with slightly  
250 different ecological interpretations. However, in West Greenland modern water  
251 samples, the occurrence of *T. kushirensis* r.s. can be linked to relatively high surface  
252 water temperatures (Krawczyk et al., 2014), hence in this study we associate higher  
253 abundance of this species with warmer surface waters.

254

### 255 **3.2.3 Benthic foraminiferal analysis**

256 *Preparation and counting method:* The benthic foraminiferal data presented  
257 here are from Lloyd et al. (2011) and Perner et al. (2011, 2013a) where details of  
258 sampling methods can be found.

259 *Ecological preferences:* Benthic foraminifera are influenced by a range of  
260 ecological parameters including factors such as food availability, nutrient content,  
261 oxygen content, water temperature and salinity (e.g. Murray, 1991; Rytter et al.,  
262 2002; Sejrup et al., 2004). Research in West Greenland has used benthic  
263 foraminifera to reconstruct variations in water mass characteristics; specifically  
264 bottom water temperature and salinity associated with variability in the WGC flow  
265 (e.g. Lloyd et al., 2005; Lloyd 2006; Perner et al., 2011, 2013a). In these studies,  
266 foraminifera with similar ecological preferences are often grouped to identify changes  
267 in the relative temperature and salinity of the WGC associated with variations in the  
268 flux of IC and EGC components to the WGC. Perner et al. (2011) identified a chilled  
269 Atlantic water group to indicate an increase in the IC contribution to the WGC (whilst  
270 chilled Atlantic water indicates some mixing of Atlantic water with a colder water  
271 mass, along the west Greenland margin this is still the warm water end member)–  
272 here we also use the dominant species from this group, *Islandiella norcrossi*,  
273 indicative of an increase in the Atlantic water component (IC) in the WGC. This  
274 species is commonly found on high latitude continental shelf environments  
275 influenced by chilled Atlantic water (e.g. Vilks, 1981; Mudie et al., 1984; Jennings  
276 and Helgadottir, 1994; Hald and Korsun, 1997; Duplessy et al., 2001; Lloyd, 2006).  
277 To identify increased influence of relatively cold, lower salinity Arctic Waters (EGC  
278 component in the WGC, or Polar Water cf. Buch, 1981) we use the Arctic water  
279 agglutinated species group identified by Perner et al. (2011) and also additional  
280 indicator species such as *Elphidium excavatum f. clavata* and *Islandiella helenae*  
281 (see Perner et al., 2011 for detailed faunal abundances). These species are able to  
282 tolerate relatively unstable, cold, lower salinity water and arctic sourced waters (e.g.  
283 Williamson et al., 1984; Schafer and Cole, 1986, Alve, 1990; Jennings and  
284 Helgadottir, 1994; Korsun and Hald, 1998). Additionally, higher abundance of *I.*  
285 *helenae* is often linked to summer ice-edge productivity in areas of seasonal sea-ice  
286 cover (e.g. Polyak and Solheim, 1994; Steinsund et al., 1994). We also use the  
287 abundance of *Nonionellina labradorica* as an indicator of increased productivity – this  
288 species is widely distributed in the North Atlantic region and is closely associated  
289 with increased flux of fresh phytodetritus to the sea floor produced by surface water  
290 productivity blooms at oceanic fronts (e.g. Cedhagen, 1991; Hald and Steinsund,  
291 1992; Hald and Korsun, 1997).

292

### 293 **3.3.4. Dinocyst analyses**

294 *Preparation and counting method:* The dinocyst data presented here are from  
295 Ouellet-Bernier et al. (2014), where details of sampling methods can be found.

296 *Ecological preferences:* The dinocysts are produced as part of the life cycle of  
297 dinoflagellates, which represent an important part of primary production together with  
298 diatoms and coccolithophorids. The organic-walled dinocysts are usually well  
299 preserved in marine sediments (e.g. de Vernal and Marret 2007 for an overview of

300 their use in paleoceanography). They represent only a fraction of original populations  
301 but reflect optimal conditions associated with reproduction. Dinocysts include both  
302 phototrophic and heterotrophic taxa. In subpolar and sea ice environments, they are  
303 particularly useful tracers as species diversity is relatively high and they are  
304 distributed depending upon several parameters including salinity, sea ice,  
305 temperature and productivity (de Vernal et al., 2013a, b). Hence, they were used to  
306 reconstruct late Quaternary sea-surface salinity, temperature and sea ice cover from  
307 sediment cores collected in northern Labrador Sea and Baffin Bay (Levac et al.,  
308 2001; de Vernal et al., 2013b; Ouellet-Bernier et al., 2014; Gibb et al., 2014).

309 Among dinocyst taxa occurring in seasonal sea ice environment, *Islandinium*  
310 *minutum* is common. It dominates quasi-exclusively together with *Brigantedinium* in  
311 areas marked by dense sea ice cover for most of the year (Buck et al., 1998; Rochon  
312 et al., 1999; de Vernal et al., 2001, 2013a). Other subpolar taxa include the cyst of  
313 *Pentapharsodinium dalei*, which is cosmopolitan and described as Arctic “warmer  
314 water” species (Dale, 1996; Rochon et al., 1999). In Disko Bugt samples, the  
315 common occurrence of *Operculodinium centrocarpum* and *Spiniferites elongatus*,  
316 which are accompanied by *Nematosphaeropsis labyrinthus* and *Spiniferites ramosus*,  
317 point to the influence of mild conditions, likely under the influence of the Atlantic  
318 water through the WGC after 7.5 ka BP (Ouellet-Bernier et al., 2014).

319

#### 320 **4. Alkenone results**

321 A number of previous studies have used  $\%C_{37:4}$  to estimate qualitative salinity  
322 changes (Rosell-Melé, 1998; Rosell-Melé et al., 2002; Sicre et al., 2002; Harada et  
323 al., 2003; Bendle et al., 2005; Blanz et al., 2005). Here, the variations in  $\%C_{37:4}$  are  
324 used as a tracer of salinity changes related to meltwater flux from the West  
325 Greenland ice sheet, since meltwater off the ice sheet is the dominant freshwater  
326 source in the region. High  $\%C_{37:4}$  levels make SST estimates based on  $U_{37}^k$  less  
327 reliable (Rosell-Melé, 1998, Bendle and Rosell-Melé, 2004). Nevertheless, given the  
328 close connection of low salinity and low temperature in meltwater plumes,  $U_{37}^k$   
329 estimates are likely to reflect qualitative temperature (SST) changes.

330 Between 8.0 and 7.5 ka BP, very high  $\%C_{37:4}$  values and low  $U_{37}^k$  suggest  
331 cold SSTs with strong ice and meltwater flux from the margins of the GIS. From 7.5  
332 to 6.5 ka BP maximum  $U_{37}^k$  and low  $\%C_{37:4}$  reflect milder SSTs and lower meltwater  
333 fluxes (Figure 2). A pronounced  $\%C_{37:4}$  increase between 6.2 and 5.5 ka BP  
334 indicates a significant oceanographic change with colder SSTs and an increase in  
335 meltwater flux at the core site. From 5.5 to 2.8 ka BP,  $\%C_{37:4}$  values decrease and,  
336 accordingly,  $U_{37}^k$  increase slightly, suggesting reduced meltwater influx and higher  
337 SST. From 2.7 to 0.8 ka BP a peak of  $\%C_{37:4}$  values corresponding to very low  $U_{37}^k$   
338 values is present in both cores 343300 and 343310 (Figure 2). This suggests  
339 increased meltwater flux and SST decrease with particularly cold SSTs at about 1.8  
340 ka BP (Figure 2). Recurring low  $\%C_{37:4}$  values and high  $U_{37}^k$  from 0.8 to 0.3 ka BP  
341 suggest meltwater flux decrease and SST warming. At site 343310, the multicore  
342 record of the last 100 years (Figure 2) displays significant increase in  $\%C_{37:4}$  values  
343 suggesting enhanced meltwater supply during the last few decades.



344

## 345 **5. Discussion**

346 The multi-proxy approach presented here, using a combination of multiple  
347 surface water proxies and a bottom water proxy obtained from the same set of  
348 samples, allows comprehensive investigation of oceanographic changes in the Disko  
349 Bugt area. In particular this combination highlights the interaction of surface and  
350 bottom (West Greenland Current) water circulation on a multi-centennial scale during  
351 the middle to late Holocene. The marine records are compared with air temperature  
352 estimates from the Camp Century ice core and from lake sediment records.

353 The multi-proxy records presented here illustrate that the different proxies do  
354 not always show the same patterns, both between the two cores and also between  
355 proxies from the same cores. There are a number of observations to be made  
356 regarding this issue. Differences between the two cores can be partly explained from  
357 their respective locations. Core 343300 was recovered from a water depth of 519 m  
358 on the southern edge of the Egedesminde Trough, while core 343310 was recovered  
359 from a water depth of 855 m from the deepest part of the trough (Figure 1). Both  
360 cores have robust chronologies and relatively consistent sedimentation rates,  
361 averaging 0.57 mm/yr in core 343300 and 2.7 mm/yr in core 343310. The lower  
362 sediment accumulation rate in core 343300 results in greater smoothing of the  
363 record (1 cm slice equates to 17.5 years) than in core 343310 (1 cm slice equates to  
364 3.7 years). The difference in smoothing might explain the generally higher amplitude  
365 of variations recorded in core 343310.

366 The high and different rates of sedimentation at the two sites suggest that a  
367 significant proportion of the sediment is not related to pelagic fluxes. A high  
368 proportion of sediment is fine grained material delivered to the depocentre of the  
369 Egedesminde Trough by ocean currents (the WGC) from the south. Hence the  
370 record of surface water proxies reconstructed from the cores presented here most  
371 likely integrates a regional south-west Greenland signal rather than reflecting local  
372 pelagic fluxes. Bottom water records based on benthic foraminifera are likely to  
373 reflect in-situ bottom water conditions but may differ because water depths of the two  
374 sites differ. Moreover, the temperature of the WGC impinging on the sea floor at the  
375 two locations is different. The core of the WGC tends to lie between 200 and 400 m  
376 (CTD profile see Figure 1 inset) hence bottom water temperatures at core 343300  
377 (519 m) are likely to be slightly higher than for core 343310 (855 m), as also  
378 indicated in Figure 3I.

379 Meltwater from land ice has a significant influence on surface water conditions  
380 in this region, as identified by the various surface water proxies. Land ice meltwater  
381 flux to this region is largely controlled by the dominant northward flowing current  
382 regime. The WGC carries meltwater delivered to the West Greenland margin from  
383 melting land based ice and tidewater glaciers along the West Greenland coastline.  
384 Hence, the surface water proxies record a meltwater signal at a regional scale.  
385 However, a significant contribution of meltwater from calving glaciers in eastern  
386 Disko Bugt to the study sites can be expected after strong glacier re-advances such

387 as during the Little Ice Age (see below). The meltwater signal may also include that  
388 of summer sea ice melt. Whatever the source, the presence of meltwater results in  
389 the development of a buoyant low salinity surface layer in summer and a strong  
390 halocline and thermocline in the photic zone (Figure 1 inset), in addition to large  
391 amplitude gradients of seasonal temperatures. This complex upper water column  
392 structure might explain differing signals recorded by biogenic tracers from the upper  
393 water layer.

394

### 395 *5.1 Middle to late Holocene oceanographic changes, atmospheric temperature and* 396 *glacier behaviour in West Greenland, in a wider North Atlantic context*

397 The full record of the past 8.3 ka BP shows trends in ocean circulation at the  
398 entrance to Disko Bugt related to variations of the WGC, surface water conditions  
399 and meltwater production. These trends broadly follow the surface air temperature  
400 proxy-record from the Camp Century ice core (Figure 3; for location of Camp  
401 Century see inset of Figure 1). This ice core location is close to the West Greenland  
402 coast and, therefore, surface air temperature changes recorded at Camp Century  
403 are likely to have been also related to changes in the oceanic conditions. The initial  
404 warming trend at the base of the Camp Century record shown in Figure 3J is an  
405 extension of the general warming trend of the early Holocene when insolation was at  
406 a maximum and the Northern Hemisphere was still recovering from the deglaciation  
407 of the mid-latitude ice sheets, though the record may also be influenced by  
408 decreasing altitude as the ice sheet thinned during the Holocene (Vinther et al.  
409 2009). The relatively cold (but warming) interval in the ice core corresponds to  
410 generally cold oceanic conditions with high meltwater flux off West Greenland  
411 (Figure 3). At Camp Century, a Holocene Thermal Maximum is recorded from ca. 6.8  
412 to 3.5 ka BP and is followed by Neoglacial cooling as evident from other ice cores  
413 (Vinther et al., 2009; Dahl-Jensen et al., 1998) and terrestrial records from West  
414 Greenland (Kaufman et al, 2004; Axford et al., 2013; Larsen et al., 2015). A  
415 significant reduction of melt water discharge in the fjords around Nuuk at about 3.2  
416 ka BP (Møller et al. 2006). This shift towards cooler conditions matches the general  
417 pattern of ocean tracers presented here (Figure 3 and 5).

418 Superimposed on the long-term trend, four distinct cold pulses of variable  
419 intensity can be identified from the Camp Century record and correspond to changes  
420 seen in our marine proxy data: i) 8.3 to 7.5 ka BP, ii) ca. 6.2 to 5.5 ka BP, iii) ca. 3.5  
421 to 2.6 ka BP, and iv) ca. 0.7 to 0.2 ka BP (grey shaded bars in Figures 3, 4 and 5).  
422 These periods also correspond to periods of glacier retreat or re-advances in West  
423 Greenland (see below). The cold pulses are generally in phase with sub-surface  
424 WGC related trends as recorded from benthic foraminifers (e.g. Figures 3H, 3I and  
425 4E, 4F), but not necessarily with the changes recorded by the surface water tracers.  
426 We relate the equivocal phase relationships to the influence of meltwater from both  
427 sea ice and land ice on surface water conditions at regional scale (discussed in more  
428 detail below; cf. also Ouellet-Bernier et al., 2014). Based on the marine proxy data

429 we divided the last 8.3 ka BP record into 8 zones (Figures 3 and 4), which reflect  
430 regional changes as discussed below:

431       Zone I: *Early Holocene, 8.3 – 7.5 ka BP*. The early part of the record is  
432 characterized by in-phase relationship of all tracers, which together indicate cold  
433 surface and sub-surface water conditions (Figure 3). Relatively cold sub-surface  
434 water conditions are recorded by the benthic foraminifera with high abundance of  
435 Arctic water foraminifera, though some variability is also present with occasional  
436 spikes in *I. norcrossi* abundance (Figure 3H, and I). This interval corresponds with  
437 cold surface water conditions as indicated by the diatom assemblage (Figure 3D)  
438 and dinocyst assemblages (Figures 3B and 3C). It is also characterised by cold  
439 surface air temperatures as recorded in the Camp Century ice core (Figure 3J). The  
440 alkenone concentrations in this interval are low. Nevertheless, the calculated values  
441 of %C<sub>37:4</sub> are relatively high (>15%, Figures 2 and 3F), suggesting that the study  
442 area was strongly influenced by enhanced meltwater supply from sea-ice or from the  
443 GIS, which is consistent with dinocyst assemblages exclusively dominated by  
444 *I. minutum* and *Brigantedinium* that reflect dense sea ice cover throughout most of  
445 the year except during a brief summer season (Ouellet-Bernier et al., 2014). An  
446 abundance peak of *N. labradorica* at ca. 7.5 ka BP (Figure 3G) suggests that the  
447 edge of the arctic sea-ice front lingered on the shelf west of Disko Bugt. Cold surface  
448 and sub-surface water conditions coincide with the final phase of deglaciation of the  
449 Laurentian ice sheet (e.g. Dyke, 2004; Jennings et al., 2015) and landward recession  
450 of the Greenland ice margins in eastern Disko Bugt (e.g. Weidick and Bennike, 2007;  
451 Young et al., 2011; Young and Briner, 2015) and along the West Greenland margin  
452 generally (e.g. Seidenkrantz et al., 2013).

453       Zone II: *Early to middle Holocene transition, 7.5 – 6.2 ka BP*. This interval is  
454 characterized by in-phase relationship of all proxies suggesting relatively warm  
455 surface and sub-surface conditions. Sub-surface water conditions are variable but  
456 generally warm as recorded by the benthic foraminifera (Figure 3I, and H), which  
457 coincides with increasing air temperatures over northwestern Greenland (Figure 3J).  
458 Surface water conditions are rather stable with little indication of melt water supply  
459 (Figure 3F), and relatively low SSTs in summer as shown by the U<sup>k</sup><sub>37</sub> (Figure 3A),  
460 dinocysts (Figures 3B, and C) and diatoms (Figure 3D). Low abundance of sea-ice  
461 associated diatoms also indicates low spring sea ice occurrence (Figure 3E)  
462 although winter sea ice was a consistent feature according to dinocyst data (Figure  
463 3C). This zone is representative of warm conditions in summer and can be  
464 associated with the delayed Holocene Thermal Maximum identified over the  
465 Canadian Arctic (e.g. Kaufman et al., 2004) and from the Greenland ice cores (e.g.  
466 Dahl-Jensen et al., 1998; Alley et al., 1999; Vinther et al., 2009) and lake records  
467 (e.g. Kaplan and Wolfe, 2006). The ice sheet margin in the Disko Bugt area had  
468 retreated to a position behind the current ice margin (e.g. Weidick and Bennike,  
469 2007; Corbett et al., 2011; Young et al., 2011, 2013b; Kelley et al., 2013; Larsen et  
470 al., 2015) as elsewhere in Greenland. A retreat of the ice sheet further from the  
471 coastline may have led to a reduced signal of regional meltwater supply preserved in  
472 our records. During this interval a relatively warmer WGC signal in the study area is

473 consistent with warm conditions in the North Atlantic and a stronger Irminger Current  
474 component to the WGC (the major source of warm water to the WGC) (e.g.  
475 Castañeda et al., 2004; Jennings et al., 2011; Olafsdottir et al., 2010).

476         Zone III: *Middle Holocene, 6.2 – 5.5 ka BP*. This interval is marked by an  
477 abrupt sub-surface cooling event as suggested by the decline of *I. norcrossi*, which is  
478 a relatively warm water benthic foraminifera, as colder water fauna such as  
479 *Islandiella helenae*, *Elphidium excavatum f. clavata* (see Perner et al., 2013a for  
480 faunal record) and other agglutinated arctic fauna (Figure 3G) increase. There is also  
481 evidence of high productivity in surface water as indicated by an increase in *N.*  
482 *labradorica* (Figure 3H) and also from productivity estimates based on dinocyst  
483 assemblages (Ouellet-Bernier et al., 2014). Increased productivity at the sea ice  
484 ('West Ice') edge close to the site is also evident by an increase in planktonic  
485 foraminifera *Neogloboquadrina pachyderma* (Perner - unpublished data). Surface  
486 waters are influenced by increase in meltwater supply as  $\%C_{37:4}$  values record an  
487 increase (Figure 3F), which is somewhat consistent with the low salinity estimates  
488 from dinocyst based reconstruction of salinity showing minimum of about 27 psu at  
489 5.5 ka BP (Ouellet-Bernier et al., 2014).. This interval coincides with an increase in  
490 sea-ice associated diatoms and reduction in relatively warm diatom flora (Figures 3D  
491 and 3E). Paradoxically, the dinocyst assemblages (Figures 3B, and C) show  
492 maximum abundance of subpolar-temperate taxa together with evidence of  
493 increased winter sea-ice, which might reflect particularly large annual amplitude of  
494 temperatures in the surface water layer then characterized by low salinity and low  
495 thermal inertia.

496         A cooling pulse is also seen in the Camp Century ice core record with a  
497 pronounced decrease of  $\delta^{18}O$  values at 5.8-5.6 ka BP (Figure 3J). It might reflect  
498 weaker and/or cooler WGC due to a southward migration of the sea ice marginal  
499 zone, which affected the local hydrography in Disko Bugt. This is compatible with  
500 increased surface water productivity due to ocean mixing and associated flux of  
501 nutrients in response to spring ice melt (e.g. Hansen et al., 1999; Levinson et al.,  
502 2000). The low isotopic excursion recorded in the Camp Century ice core after 6 ka  
503 BP is likely linked to the temporary cooling-freshening in oceanic conditions affecting  
504 northeast Baffin Bay. The colder WGC conditions may well be related to a cooling  
505 identified in the East Greenland Current at about this time (Müller et al., 2012; Ran et  
506 al., 2006), and to a marked temperature drop in the northern North Atlantic (e.g.  
507 Moros et al., 2004, Telesiński et al., 2014) that is likely linked to the most  
508 pronounced North Atlantic Holocene IRD event (Bond et al., 2001).

509         Zone IV: *Middle Holocene, 5.5 – 3.5 ka BP*. This zone is marked by a return to  
510 relatively warm sub-surface conditions (Figure 3I). Diminishing  $\%C_{37:4}$  values suggest  
511 a gradual decrease of meltwater influence (Figure 3F). Diatom and dinocyst  
512 assemblages both show relatively mild surface water despite a gradual trend  
513 towards cooler conditions (diatoms - Figure 3D, dinocysts – Figures 3B and 3C). The  
514 reduction in *N. labradorica* indicates lower surface water productivity (Figure 3G) as

515 also reconstructed based on dinocyst assemblages (Ouellet-Bernier et al., 2014).  
516 This, combined with the reduced meltwater influence, suggests that the productive  
517 ice edge frontal zone had migrated further north. This migration could be due to the  
518 increased strength and/or warmth of the WGC but may have been further influenced  
519 by changes in meltwater flow and the end of ice blocking of the Vaigat Strait at ca.  
520 6.0 ka BP (Perner et al., 2013b), leading to an increased iceberg flux northwards  
521 through the Vaigat rather than westwards across the Disko Bugt shelf (Figure 1).

522 The relatively warm oceanic conditions during this time also correspond to  
523 relatively warm air temperatures (e.g. Camp Century ice core, Figure 3J). Several  
524 lake records near Jakobshavn Isbræ display high loss on ignition values  
525 representing high productivity under relatively warm terrestrial conditions and  
526 relatively high chironomid-based temperature reconstructions from one of the Lakes,  
527 North Lake (Axford et al., 2013). High lake levels linked to warmer conditions are  
528 also reported in the Kangerlussuaq region, just south of Disko Bugt (Aebly and Fritz,  
529 2009). Geomorphological studies in the eastern Disko Bugt area report a largely  
530 land-based ice sheet and reduced meltwater runoff from the GIS after 6 ka BP  
531 (Briner et al., 2010; Weidick and Bennicke, 2007; Weidick et al., 1990). Briner et al.  
532 (2015) also reconstruct minimum ice extent from c. 5 – 3 ka BP based on a  
533 chronology from reworked shells. A strong and relatively warm IC likely causing the  
534 warm/strong WGC is reported from the East Greenland shelf (Jennings et al., 2002,  
535 2011) and southwest and south of Iceland (e.g. Knudsen et al., 2008b; Olafsdottir et  
536 al., 2010).

537 *Zone V: Middle to late Holocene transition, 3.5 - 2.6 ka BP.* This zone is  
538 characterized by a shift toward cooler conditions as shown by some proxies. The  
539 warm sub-surface water conditions of the previous zone end with a rather abrupt  
540 decrease of *I. norcrossi* in benthic foraminifera assemblages at ca. 3.5 ka BP  
541 (Figures 3H and 3I; Perner et al., 2013a, also show an increase in other arctic  
542 foraminifera such as *Elphidium excavatum* f. *clavata* at this time). The sub-surface  
543 cooling coincides with very low %C<sub>37:4</sub> values (Figure 3F) the occurrence of cold  
544 diatom assemblages (Figure 3D), with increasing sea-ice species (Figure 3C).  
545 Cooling is also recorded from the Camp Century ice core record (Figure 3J).

546 This cold period differs from the one identified in zone III by having no  
547 indication of meltwater supply. This cool episode recorded in the archives from Disko  
548 Bugt and the wider West Greenland terrestrial archives appears to be the  
549 culmination of a longer climate cooling trend in the North Atlantic (Wanner et al.,  
550 2011). The cooling of the WGC most likely results from a weaker IC and/or stronger  
551 EGC and coincides with the beginning of Neoglaciation as shown by IRD deposition  
552 off southeast Greenland (e.g. Andersen et al., 2004, Jennings et al., 2002, 2011;  
553 Jiang et al., 2002). Colder oceanic and atmospheric conditions led to an advance of  
554 land based ice marking the initial phase of the Neoglacial (Briner et al., 2011;  
555 Weidick and Bennike, 2007; Young et al., 2011). This is in line with relatively low  
556 meltwater production. A marked reduction in meltwater discharge at ca. 3.2 ka BP  
557 has also been documented in a southwest Greenland fjord (Møller et al., 2006).

558 Colder and dryer conditions are also indicated by relatively low lake levels in the  
559 Kangerlussuaq area (Aebly and Fritz, 2009) and decreased LOI values from lakes in  
560 the Disko Bugt area reflecting low primary productivity (Axford et al., 2013).

561         Zone VI: *Late Holocene, 2.6 - 0.7 ka BP*. Oceanic conditions during this  
562 period were highly variable. The first part of this zone from 2.6 to 1.7 ka BP is  
563 characterized by centennial scale fluctuations and general warming of sub-surface  
564 waters (Figures 4E and 4F). The meltwater influence identified from %C<sub>37:4</sub> values is  
565 also variable, but overall increases to relatively stable and high levels from ca. 2 ka  
566 BP (Figure 4D). The diatom flora suggest surface waters initially warm in phase with  
567 sub-surface waters until 1.7 ka BP (Figure 4B), however, the dinocyst assemblage  
568 shows a continuation of the gradual cooling trend from the previous zone culminating  
569 in cool conditions at about 1.5 ka BP (Figures 3B and 3C; see also reconstructions in  
570 Ouellet-Bernier et al., 2014). Benthic foraminifera then record gradual cooling of sub-  
571 surface waters, but with centennial scale fluctuations superimposed on the longer  
572 term cooling. This trend culminates in cold conditions from 0.7 ka BP during the LIA  
573 (Figures 4E and 4F). The diatom flora show highly variable conditions from 1.6 ka  
574 BP onwards and a trend of increasing sea ice-associated flora reaching a peak at  
575 the end of this zone (Figures 4B and 4C). An expansion of sea ice is supported by  
576 data from the fjords around Nuuk, more to the south, where a marked increase of  
577 sea ice occurred and regional lake records indicate significant cooling shortly after  
578 0.8 ka BP (Kuijpers et al. 2014).

579         The initial warming in sub-surface conditions from 2.6 to 1.6 ka BP coincides  
580 with a slight increase in  $\delta^{18}\text{O}$  in the Camp Century ice core (Figure 4G). The  
581 variability in the sub-surface WGC record is generally consistent with centennial  
582 scale climate changes from the eastern North Atlantic region, such as the Roman  
583 Warm Period (RWP), Dark Ages (DA), Medieval Climate Anomaly (MCA) and Little  
584 Ice Age (LIA) (Figure 4). The WGC and the atmospheric conditions in West  
585 Greenland seem closely coupled to the oceanographic changes in other areas of the  
586 North Atlantic, such as the Reykjanes Ridge, where a pronounced warming pulse is  
587 also recorded at ca. 2 ka BP (Moros et al., 2012). There is a peak of relatively warm  
588 sub-surface water from ca. 1.8 to 1.65 ka BP that occurs during a period of  
589 increased %C<sub>37:4</sub> values that could relate to high meltwater flux. This time interval  
590 corresponds to the RWP, which is the warmest period of the late Holocene recorded  
591 at our sites. The influence of relatively warm oceanic conditions at ca. 2 ka BP were  
592 also reported based on sedimentological proxies from Narsaq Sound, southwest  
593 Greenland (Norgaard-Pedersen and Mikkelsen, 2009). Increased meltwater release  
594 most likely results from WGC-induced melting of marine-based outlet glaciers and  
595 icebergs after the ice sheet margin had re-advanced and major glaciers extended  
596 again into the fjords during Neoglacial cooling. The period from 1.3 ka BP (coinciding  
597 with the MCA) marks a transitional period with gradually cooling sub-surface waters,  
598 highly variable meltwater flux, sea-ice cover and sea surface conditions.

599         The period after ca. 2.0 ka BP, when meltwater flux was at a maximum,  
600 seems to be characterized by particularly harsh terrestrial conditions in the Disko

601 Bugt area. Weidick and Bennike (2007) report youngest ages from lakes in  
602 southeast Disko Bugt of ca. 2.2 ka BP, indicating limited sedimentation thereafter  
603 and lakes near Jakobshavn Isbræ also show very low accumulation from this time  
604 onwards (Axford et al., 2013) which could reflect nearly year-round frozen conditions.  
605 The high meltwater flux initiated by the strong sub-surface ocean warming may have  
606 contributed to a rather moderate atmospheric temperature warming recorded at  
607 Camp Century around 2 ka BP. After ca. 1.0 ka BP, with transition into the LIA, sub-  
608 surface waters continue to cool, while surface waters show a clear warming. Diatom  
609 (Figure 4B) and dinocyst floras both show this warming (Figure 3C and core 343310,  
610 Ribeiro et al., 2012; Ouellet-Bernier et al., 2014). This transition to an anti-phase  
611 relationship most likely reflects a marked hydrographic variability (Krawczyk et al.,  
612 2013) related to a regionally unstable climate regime (e.g. increased storminess and  
613 enhanced mixing of water masses).

614 Zone VII: Late Holocene, 0.7 – 0.2 ka BP. A clear cooling is seen in sub-  
615 surface waters during this interval (Figures 4E and 4F), correlating with cold  
616 atmospheric conditions seen in the Camp Century ice core (Figure 4G). In contrast  
617 surface water conditions are characterized by a relative warming (Figure 4B) along  
618 with a decrease in sea-ice occurrence from a peak at the beginning of this interval  
619 (Figure 4C). Ribeiro et al. (2012) present dinocyst assemblages covering this period  
620 showing warming at the beginning but cooling from c. 0.5 ka BP until 0.1 ka BP.  
621 Meltwater influence is low during this interval (Figure 4D). Benthic foraminifera  
622 suggest sub-surface conditions during this period were colder than the rest of the  
623 record, with the exception of zone 1 (Figures 3G and 3H). One significant difference  
624 with this earlier cooling event, however, is the out-of-phase relationship with surface  
625 water conditions in Zone VII.

626 The timing of Zone VII corresponds closely with the LIA. The significant  
627 advance of the GIS and outlet glaciers in the Disko Bugt area at this time (Briner et  
628 al., 2010; Young et al., 2011) and low lake levels in the Kangerlussuaq region (Aebly  
629 and Fritz, 2009) may have been caused by a combination of the cold oceanic and  
630 atmospheric conditions in the area corresponding to the LIA. Relatively cold sub-  
631 surface waters (reflecting a cool WGC) led to the reduced meltwater influx by melting  
632 of icebergs/outlet glaciers and sea-ice at this time. This lack of meltwater has been  
633 invoked to explain the increase in SST identified from the diatom flora (Figure 4B,  
634 Krawczyk et al., 2010) and, may also explain the initial warm dinocyst flora (Ribeiro  
635 et al., 2012). The reduced meltwater flux may also explain the slight decrease in sea-  
636 ice associated diatoms during this period – though sea-ice is still present (Figure  
637 4C).

638 Zone VIII: 20<sup>th</sup> Century. Sub-surface water conditions over the last 100 years,  
639 in the context of the preceding conditions, remain relatively cold (Figure 4E, F and  
640 5C). However, there is a slight warming in sub-surface conditions, particularly since  
641 AD 2000, as discussed in more detail in Lloyd et al. (2011), which is accompanied  
642 by a significant increase in meltwater production (Figure 4D). The minor sub-surface  
643 ocean warming is also demonstrated by instrumental data over recent decades and

644 correlates with a significant retreat of the tidewater calving margin of Jakobshavns  
645 Isbrae. The historical retreat of the calving margin of Jakobshavns Isbrae during the  
646 20<sup>th</sup> Century is well constrained and coincides with a period of significant increase in  
647 %C<sub>37:4</sub>, the alkenone based meltwater proxy, supporting our interpretation of this  
648 proxy from our records. This also corresponds to low SST estimates based on the  
649 alkenone data (Figure 3A) also supporting our interpretation of increased meltwater  
650 production leading to colder surface water temperatures earlier in the records  
651 presented here. This highlights the sensitivity of the ice margin to relatively small  
652 changes in ocean forcing. As discussed in Lloyd et al. (2011), the conditions in Disko  
653 Bugt correlate well with broader North Atlantic conditions as recorded in the Atlantic  
654 Multidecadal Oscillation (Gray et al., 2004) and the Arctic-wide surface air  
655 temperature anomaly from Polyakov et al. (2002).

656

## 657 *5.2. Linking environmental changes to the history of human occupation in West* 658 *Greenland*

659 The cultural history of Greenland began 4.5 ka BP with the immigration of the  
660 Saqqaq from high Arctic North America. The history of human occupation in  
661 Greenland is characterized by arrival and disappearance of several cultures rather  
662 than continuous human settlement. It has been suggested that environmental  
663 change was the major cause for this pattern (McGovern, 1991; McGhee, 1996;  
664 Jensen, 2006). In Disko Bugt, numerous dwellings and artifacts have been  
665 recovered from the Saqqaq and Dorset people who inhabited the region between 4.5  
666 and/3.4 ka BP and 2.8 - 2.2 ka BP, respectively (Jensen et al., 1999; Jensen 2006).

667 Based on the oceanographic and climatic inferences presented here the  
668 Saqqaq settled in West Greenland during a time of relatively mild conditions towards  
669 the end of the Holocene Thermal Maximum, when only winter sea-ice cover  
670 prevailed. Such an environment agrees well with the archaeological records that  
671 describe the Saqqaq people as preferential open water hunters (e.g. Meldgaard,  
672 2004; Jensen, 2006). In the later period of their settlement, the proxy records  
673 indicate increasing climate instability and cooling. Excavations from Qeqertasussuk  
674 in Sydostbugten have shown that from 4.2 to 3.5 ka BP this site was inhabited  
675 primarily in spring and summer, which was the season when harp seal was the  
676 primary game (e.g. Meldgaard, 2004; Jensen, 2006). The environmental change to  
677 colder and more unstable conditions we reconstruct after ca. 3.5 ka BP (Figure 4) is  
678 likely to have affected their food source and supports the view that the Saqqaq  
679 people left Disko Bugt due to deteriorating climatic conditions (Meldgaard, 2004).

680 While the link between appearance/disappearance of the Saqqaq culture to  
681 environmental changes appears straightforward (e.g. Meldgaard, 2004; Jensen,  
682 2006; Moros et al., 2006; D'Andrea et al., 2011), the influence of environmental  
683 changes on the Dorset culture is not entirely clear (e.g. D'Andrea et al., 2011). The  
684 Dorset people were better adapted to sea ice hunting than the Saqqaq (Jensen,  
685 2006). The oldest records of Dorset occupation provide a date of about 2.8 ka BP  
686 (Jensen et al., 1999) and coincide with cool sea and air temperatures and relatively  
687 extended sea ice cover evident from our marine records (see Figure 4).



688 From ca. 2.7 ka BP a shift in environmental conditions took place in the Disko  
689 Bugt area with increasing temperatures in sub-surface and surface waters (i.e. by  
690 diatom flora) together with indications for increased freshwater (meltwater) input  
691 (Figures 4C and 4E) and low sea-surface salinity (Ouellet-Bernier et al., 2014). A  
692 progressive warming at this time is also noted from dinocyst-based reconstruction in  
693 Disko Bugt (Ouellet-Bernier et al., 2014), and at the Kangerlussuaq lake from  
694 alkenones (D'Andrea et al., 2011) and further south along the Greenland margin  
695 from sedimentological data (Nørgaard-Pedersen and Mikkelsen, 2009). Moros et al.  
696 (2006) argued that the inferred warm sea-surface temperatures and limited sea ice in  
697 the Disko Bugt region were unfavorable to the Dorset, given that they were  
698 predominantly sea-ice hunters. Archaeological evidence (Jensen, 2006) provides  
699 three key pieces of information: (i) the latest population is noted in West Greenland  
700 at ca. 2.2 ka BP, (ii) in some areas Dorset food is dominated by caribou, indicating  
701 that the living resource base was diverse and not solely tied to sea-ice hunting; (iii)  
702 there is no northward migration of the Dorset at this time, which would seem likely  
703 during warming over West Greenland. Combining the archaeological evidence with  
704 the inferences from the new marine proxy data there appears to be a plausible  
705 alternative to the warming link proposed by Moros et al. (2006). The drop in  
706 temperature after 2 ka BP and associated harsh conditions on land (see above) may  
707 have had a negative effect on terrestrial living resources and thus may have been  
708 another factor that forced the Dorset to leave the area.

709 The Norse migrated to West Greenland at about 1.0 ka BP, which  
710 corresponds to a time of transition recorded by all proxies that suggest a shift  
711 towards warm conditions in surface waters. The abandonment of the Western  
712 Settlement of the Norse at about 0.65 ka BP could be linked to climate deterioration  
713 evident from sub-surface ocean and Greenland air temperatures accompanied by  
714 significant glacier advances and sea ice expansion, which in West Greenland waters  
715 started already shortly after 0.8 ka BP (e.g. Kuijpers et al., 2014).

716

## 717 **6. Conclusions**

718 The multi-proxy approach adopted here identifies the complex nature of the  
719 changes in ocean circulation and interaction between surface and sub-surface  
720 waters and also with the ice margin history of the GIS. We document broad scale  
721 coherent patterns in the interaction between the relatively warm WGC and surface  
722 conditions that are influenced by freshwater and meltwater discharge from the GIS.  
723 Increases in meltwater flux may lead to highly stratified upper water masses and  
724 large amplitude gradients of seasonal temperature and sea-ice cover. Therefore,  
725 atmospheric warming and/or enhanced strength of the WGC that may accelerate the  
726 melt of the ice margins result in low surface salinity, cooling and sharp stratification  
727 in the upper water masses. This will also influence surface water temperature,  
728 salinity, seasonality, sea ice extent, productivity, and timing of surface water algal  
729 blooms. This, of course, complicates the interpretation of proxy data, which may

730 capture different signals related to climate changes, e.g. depending on where in the  
731 water column the signal were acquired.

732 The overall records show high frequency variations superimposed on longer-  
733 term trends. The combination of different records help to identify key changes in  
734 benthic and pelagic environments related to large-scale climate changes. One  
735 striking feature is the linkage that may be established between the sub-surface water  
736 conditions (benthic foraminifera), the atmospheric temperature (Camp Century ice  
737 core) and the surface water conditions based on North Atlantic-associated dinocysts.  
738 The coherency of the long-term changes captured by these independent sets of data  
739 points to consistent vectors and strength in the atmospheric circulation and ocean  
740 circulation patterns. They all show that in the Disko Bugt region the onset of  
741 postglacial circulation pattern occurred at about 7.5 ka BP, with an optimum in the  
742 warm Atlantic component until about 4 ka BP. From 4 ka BP a general cooling  
743 started as a regional signature of the middle to late Holocene cooling.

744 Beyond the above mentioned general trends, variations in the marine proxies  
745 record local to regional changes resulting from large scale climate events influencing  
746 ocean circulation, but also from more local effects of meltwater discharges from the  
747 GIS margins. Several phases can be distinguished, as summarized below (Figure 5).

748 An early postglacial phase from 8.5 to 7.5 ka BP. This period is strongly  
749 influenced by the deglaciation of the Laurentide Ice Sheet and southern margins of  
750 the GIS, which together resulted in significant meltwater flux in Baffin Bay and along  
751 the West Greenland margin and led to variable but predominantly cold ocean and  
752 dense sea ice cover (Figure 5).

753 The following period from about 7.5 to 3.5 ka BP corresponds to the regional  
754 Holocene Thermal Maximum as identified from terrestrial records in the West  
755 Greenland - Baffin Island area by Kaufman et al. (2004). This interval is  
756 characterized by relatively mild air and ocean conditions (Figures 5) and GIS  
757 margins more inland than the current position (e.g. Kelley et al., 2013; Larsen et al.,  
758 2015). During this interval, the influence of meltwater may have remained low due to  
759 the inland position of the ice margin, but apparently increased during a period of  
760 relatively cold bottom waters and an air temperature cooling in west Greenland (5.9  
761 – 5.7 ka BP, Figure 5). This increase in meltwater could be the response to a re-  
762 advance of the ice margin and ice flux from tidewater glaciers along the west  
763 Greenland coast. The warmest conditions in west Greenland in the ocean (WGC and  
764 surface waters) and atmosphere appear to occur between 5.5 and 4 ka BP (Figure  
765 5). The Saqqaq culture colonized the area at ca. 4.5 ka BP towards the end of this  
766 period, probably taking advantage of the relatively mild conditions.

767 Late Holocene cooling after ca. 3.5 ka BP leading to re-advance of the ice  
768 margins (e.g. Kelly 1980) marks the end of the Holocene Thermal Maximum on a  
769 regional scale and coincides with Neoglacial ice advance (Figure 5). The onset of  
770 offshore cooling identified in our records coincides with the disappearance of the  
771 Saqqaq culture from West Greenland. The last 3500 years were apparently marked  
772 by large amplitude oscillations with regard to bottom and surface water conditions.  
773 Alternation of very cold (3.5-2.7 ka BP) and milder (2.7-1.2 ka BP) conditions are

774 most likely linked to variations in meltwater discharge and the advance of tidewater  
775 glaciers along the West Greenland margin (Figure 5). During the episodes of  
776 advanced ice margin, meltwater discharge and unstable coastal conditions prevailed.  
777 These variable conditions are likely to have had an impact on the history of human  
778 occupation along the West Greenland coastline. While it is still unclear what the key  
779 drivers influencing human occupation of West Greenland are, our records highlight  
780 clear changes in the offshore environment during this period of changing human  
781 settlement. The Dorset arrived during a relatively cold interval, and their  
782 disappearance at ca. 2.2 ka BP may have been related to harsh coastal conditions.  
783 The Norse culture arrived during the relatively mild conditions of the MCA, and  
784 seems to have also disappeared because of harsh conditions at the onset of the LIA  
785 (Figure 5).

786 The multi-proxy approach discussed here sheds light on the interaction  
787 between the oceans, atmosphere and the GIS and identifies the complex influence  
788 of the ocean on glacial behaviour in the West Greenland region. Oceanographic  
789 conditions may also have been important for the history of human occupation.

790

## 791 **Acknowledgements**

792 The authors wish to thank Captain and Crew of the R/V Maria S. Merian for their  
793 excellent work during cruise MSM05/03. Furthermore, we thank the Deutsche  
794 Forschungsgemeinschaft (DFG) for funding the project 'Disco Climate' (MO1422/2-1)  
795 and 'GREENClimate' (PE2071/2-1). Funding from Polish National Centre in Cracow  
796 grant no. 2011/03/N/ST10/05794 (DK and AW) is acknowledged. We would also like  
797 to thank two anonymous reviewers for their constructive reviews of this manuscript.

798

## 799 **References**

- 800 Aebly, F., Fritz, S.C. 2009. Paleohydrology of Kangerlussuaq (Søndre Strømfjord),  
801 West Greenland during the last ~8000 years. *The Holocene*, 19, 91–104.
- 802 Alley, R.B., Agustsdottir, A.M., and Fawcett, P.J. 1999. Ice-core evidence of late-  
803 Holocene reduction in North Atlantic Ocean heat transport. *Geophysical*  
804 *Monograph*, 112, 301–312.
- 805 Alve, E. 1990. Variations in estuarine foraminiferal biofacies with diminishing  
806 oxygen conditions in Drammensfjord. SE Norway. In: Hemleben, C., Kaminski, M.  
807 A., Kuhnt, W., and Scott, D. B. (eds.), *Paleoecology, Biostratigraphy,*  
808 *Paleoceanography and Taxonomy of Agglutinated Foraminifera: NATO AS1*  
809 *Series., Series C, Mathematical and Physical Sciences, Kluwer Academic*  
810 *Publishers, Dordrecht*, 327, 661-694.
- 811 Andersen, O.G.N. 1981. The annual cycle of temperature, salinity, currents and  
812 water masses in Disko Bugt and adjacent waters, West Greenland.  
813 *Meddelelserom Grønland. Bioscience*, 5, 1-36.

814 Andersen, C., Koc, N., Jennings, A., et al. 2004. Nonuniform response of the major  
815 surface currents in the Nordic Seas to insolation forcing: Implications for the  
816 Holocene climate variability. *Paleoceanography*, 19, PA2003, doi:  
817 10.1029/2002PA000873.

818 Andresen, C.S., Sicre, M.-A., Straneo, F., Sutherland, D.A., Schmith, T., Ribergaard,  
819 M.H., Kuijpers, A., Lloyd, J.M. 2013. A 100-year record of alkenone-derived SST  
820 changes by Southeast Greenland. *Continental Shelf Research*, 71, 45-51.

821 Axford, Y., Losee, S., Briner, J.P., Francis, D.R., Langdon, P.G., and Walker, I.R.  
822 2013. Holocene temperature history at the western Greenland Ice Sheet margin  
823 reconstructed from lake sediments. *Quaternary Science Reviews*, 59, 87–100.

824 Bâcle, J.E., Carmack, C., Ingram, R.G. 2002. Water column structure and  
825 circulation in the North Water during spring transition: April-July 1998. *Deep Sea*  
826 *Research*, 49, 4907-4925.

827 Bendle, J., Rosell-Melé, A., Ziveri, P. 2005. Variability of unusual distribution of  
828 alkenones in the surface waters of the Nordic seas. *Paleoceanography*, 20,  
829 PA2001, doi:2010.1029/2004PA001025.

830 Bendle, J., Rosell-Melé, A. 2004. Distributions of UK37 and UK37' in the surface  
831 waters and sediments of the Nordic Seas: Implications for paleoceanography.  
832 *Geochemistry, Geophysics, Geosystems*, 5.

833 Bindschadler, R.A. 1984. Jakobshavns Glacier drainage basin; a balance  
834 assessment. *Journal of Geophysical Research, C. Oceans and Atmospheres*, 89,  
835 2066-2072.

836 Blanz, T., Emeis, K.C., Siegel, H. 2005. Controls on alkenone unsaturation ratios  
837 along the salinity gradient between the open ocean and the Baltic Sea.  
838 *Geochimica et Cosmochimica Acta*, 69, 3589–3600.

839 Bond, G., Kromer, B., Beer, J., et al. 2001. Persistent solar influence on North  
840 Atlantic climate during the Holocene. *Science*, 294, 2130–2136.

841 Brassell, S.C., Eglinton, G., Marlowe, I.T., Pflaumann, U., Sarnthein, M. 1986.  
842 Molecular stratigraphy: a new tool for climatic assessment. *Nature*, 320, 129-133.

843 Briner, J.P., Stewart, H.A.M., Young, N.E., Philipps, W., Losee, S. 2010. Using  
844 proglacial-threshold lakes to constrain fluctuations of the Jakobshavn Isbræ ice  
845 margin, western Greenland, during the Holocene. *Quaternary Science Reviews*,  
846 29, 3861-3874.

847 Briner, J.P., Kaufman, D.S., Bennike, O., Kosnik, M.A. 2014. Amino acid ratios in  
848 reworked marine bivalve shells constrain Greenland Ice Sheet history during the  
849 Holocene. *Geology*, 42, 75-78.

850 Briner, J.P., Young, N.E., Thomas, E.K., Stewart, H.A.M., Losee, S., Truex, S., 2011,  
851 Varve and radiocarbon dating support the rapid advance of Jakobshavn Isbræ  
852 during the Little Ice Age. *Quaternary Science Reviews*, 30, 2476–2486.

853 Bronk Ramsey, C., 2009. Bayesian analysis of radiocarbon dates. *Radiocarbon* 51,  
854 pp. 337.

855 Buch, E., Pedersen, S.A., Ribergaard, M.H. 2004. Ecosystem Variability in West  
856 Greenland Waters. *Journal of Northw. Atl. Fish. Sci.*, 34, 13-28.

- 857 Buch, E., 1981. A Review of the oceanographic conditions in subarea O and 1 in the  
858 decade 1970- 79. NAFO Symposium on Environmental conditions in the  
859 Northwest Atlantic during 1970-79. *NAFO Scientific Council Studies*, 5.
- 860 Buck KR, Nielsen TG, Hansen BW et al., 1998. Infiltration phyto- and  
861 protozooplankton assemblages in the annual sea ice of Disko Island, West  
862 Greenland, spring 1996. *Polar Biology*, 20, 377–381.
- 863 Castañeda, I., Smith, L.M., Kristjánsdóttir, G.B., Andrews, J.T. 2004. Temporal  
864 changes in Holocene  $\delta^{18}\text{O}$  records from the northwest and central North Iceland  
865 Shelf. *Journal of Quaternary Science*, 19, 321-334.
- 866 Cedhagen, T. 1991. Retention of chloroplasts and bathymetric distribution in the  
867 sublittoral foraminifera *Nonionellina labradorica*. *Ophelia*, 33, 17–30.
- 868 Corbett, L.B., Young, N.E., Bierman, P.R., Briner, J.P., Neumann, T.A., Rood, D.H.,  
869 Graly, J.A. 2011. Paired bedrock and boulder  $^{10}\text{Be}$  concentrations resulting from  
870 early Holocene ice retreat near Jakobshavn Isfjord, western Greenland.  
871 *Quaternary Science Reviews*, 30, 1739-1749.
- 872 Cuny, J., Rhines, P.B., Niiler, P.P., Bacon, S. 2002. Labrador Sea boundary  
873 currents and the fate of Irminger Sea Water. *Journal of Physical Oceanography*,  
874 32, 627-647.
- 875 Dahl-Jensen, D., Mosegaard, K., Gundestrup, N., Clow, G. D., Johnsen, S. J.,  
876 Hansen, A. W., Balling, N. 1998. Past temperatures directly from the Greenland  
877 ice sheet. *Science*, 282, 268-271.
- 878 Dale, B. 1996. Dinoflagellate cyst ecology: Modeling and geological applications.  
879 *Palynology: Principles and Applications*, 3, 1249–1275.
- 880 D’Andrea, W.J., Huang, Y., Fritz, S., Anderson, N.J. 2011. Abrupt Holocene climate  
881 change as an important factor for human migration in West Greenland. *PNAS*,  
882 108, 9765-9769.
- 883 de Vernal, A., Bilodeau, G., Henry, M. 2010. Micropaleontological Preparation  
884 Techniques and Analyses. Cahier du Geotop n\_3,  
885 <http://www.geotop.ca/en/publications/cahiers-de-laboratoire-et-protocoles.html>
- 886 de Vernal, A., et al. 2001. Dinoflagellate cyst assemblages as tracers of sea-surface  
887 conditions in the northern North Atlantic, Arctic and sub-Arctic seas: the new “n =  
888 677” database and application for quantitative paleoceanographical reconstruction.  
889 *Journal of Quaternary Science*, 16, 681-699.
- 890 de Vernal, A., Rochon, A., Fréchette, B., Henry, M., Radi, T., Solignac, S. 2013a.  
891 Reconstructing past sea ice cover of the Northern hemisphere from dinocyst  
892 assemblages : status of the approach. *Quaternary Science Reviews*, 79,122-134.
- 893 de Vernal, A., Hillaire-Marcel, C., Rochon, A., Fréchette, B., Henry, M., Solignac, S.,  
894 Bonnet, S. 2013b. Dinocyst-based reconstructions of sea ice cover concentration  
895 during the Holocene in the Arctic Ocean, the northern North Atlantic Ocean and its  
896 adjacent seas. *Quaternary Science Reviews*, 79, 111-121.
- 897 de Vernal, A., Marret, F. 2007. Organic-walled dinoflagellates : tracers of sea-surface  
898 conditions, In C. Hillaire-Marcel and A. de Vernal (eds.) *Proxies in Late Cenozoic*  
899 *Paleoceanography*, Elsevier, pp. 371-408.

900 Duplessy, J-C., Invanova, E.V., Murdmaa, I.O, Paterne, M., and Labyrie, L., 2001.  
901 Holocene palaeoceanography of the northern Barents Sea and variations of the  
902 northward heat transport by the Atlantic Ocean. *Boreas*, 30, 2-16.

903 Dyke, A.S. 2004. An outline of the deglaciation of North America with emphasis on  
904 central and northern Canada. In: Ehlers, J., Gibbard, P.L. (Eds.), Quaternary  
905 Glaciations, Extent and Chronology. Part II. North America, Developments in  
906 Quaternary Science, vol. 2b. Elsevier, Amsterdam

907 Fredskild, B. 1996. Holocene climatic changes in Greenland. Bjarne Grønøw (ed.).  
908 The Paleo-Eskimo cultures of Greenland, 244-251. Dansk Polar Center.

909 Fryxell G.A. 1975. Morphology, taxonomy, and distribution of selected diatom  
910 species of *Thalassiosira* Cleve in the Gulf of Mexico and Antarctic waters. Ph.D.  
911 Thesis, Texas A & M University, United States of America.

912 Gibb, O.T., Hillaire-Marcel, C., de Vernal, A. 2014. Oceanographic regimes in the  
913 northwest Labrador Sea since Marine Isotope Stage 3 based on dinocyst and  
914 stable isotope proxy records. *Quaternary Science Reviews*, 92, 269-279.

915 Gray, S.T., Graumlich, L.J., Betancourt, J.L., Pederson, G.T. 2004. A tree-ring based  
916 reconstruction of the Atlantic Multidecadal Oscillation since 1567 A.D.  
917 *Geophysical Research Letters*, 31, L12205, doi:10.1029/2004GL019932.

918 Hald, M., Korsun, S. 1997. Distribution of modern benthic foraminifera from fjords of  
919 Svalbard, European Arctic. *Journal of Foraminiferal Research*, 27, 101–122.

920 Hald, M., Steinsund, P.I. 1992. Distribution of surface sediment benthic  
921 foraminifera in the southwestern Barents Sea. *Journal of Foraminiferal Research*,  
922 21, 347–62.

923 Hansen, B.W., Nielsen, T.G., Levinsen, H. 1999. Plankton community structure and  
924 carbon cycling on the western coast of Greenland during the stratified summer  
925 situation. III. Mesozooplankton. *Aquatic Microbial Ecology*, 16, 233-249.

926 Harada, N., Shin, K.H., Murata, A., Uchida, M., and Nakatani, T. 2003.  
927 Characteristics of alkenones synthesized by a bloom of *emiliania huxleyi* in the  
928 Bering Sea. *Geochim. Cosmochim. Acta*, 67, 1507–1519.

929 Hasle, G.R., Syvertsen, E.E. 1996. Marine diatoms. In: Tomas, C.R. (Ed.),  
930 Identifying Marine Diatoms and Dinoflagellates. Academic Press, San Diego, pp.  
931 5-386.

932 Holland, D.M., Thomas, R.H., De Young, B., Ribergaard, M.H., Lyberth, B. 2008.  
933 Acceleration of Jakobshavn Isbrae triggered by warm sub-surfaceocean waters.  
934 *Nature Geoscience*, 1, 659-664.

935 Howat, I.M., Joughin, I., Scambos, T.A. 2007. Rapid changes in ice discharge from  
936 Greenland outlet glaciers. *Science*, 315, 1559-1561.

937 Howat, I.M., Joughin, I., Fahnestock, M., Smith, B.E., Scambos, T.A. 2008.  
938 Synchronous retreat and acceleration of southeast Greenland glaciers 2000-06:  
939 ice dynamics and coupling to climate. *Journal of Glaciology*, 54, 646-660.

940 Howat, I.M., Ahn, Y., Joughin, I., van den Broeke, M.R., Lenaerts, J.T.M., Smith, B.  
941 2011. Mass balance of Greenland's three largest outlet glaciers, 2000-2010.  
942 *Geophysical Research Letters*, 38.

- 943 Jakobsson, M., Macnab, R., Mayer, M., Anderson, R., Edwards, M., Hatzky, J.,  
 944 Schenke, H-W., Johnson, P. 2008. An improved bathymetric portrayal of the Arctic  
 945 Ocean: Implications for ocean modeling and geological, geophysical and  
 946 oceanographic analyses, v. 35, L07602, *Geophysical Research Letters*,  
 947 doi:10.1029/2008GL033520.
- 948 Jennings, A.E., Helgadottir, G. 1994. Foraminiferal assemblages from the  
 949 fjords and shelf of eastern Greenland. *Journal of Foraminiferal Research*, 24,  
 950 123–44.
- 951 Jennings, A.E., Knudsen, K.L., Hald, M., Hansen, C.V., Andrews, J.T. 2002. A mid-  
 952 Holocene shift in Arctic sea-ice variability on the East Greenland Shelf. *The*  
 953 *Holocene*, 12, 49-58.
- 954 Jennings, A.E., Andrews, J., Wilson, L. 2011. Holocene environmental evolution of  
 955 the SE Greenland Shelf North and South of the Denmark Strait: Irminger and East  
 956 Greenland current interactions. *Quaternary Science Reviews*, 30, 980-998.
- 957 Jennings, A.E., Walton, M.E., Ó Cofaigh, C., Kilfeather, A., Ortiz, J., de Vernal, A.,  
 958 Dowdeswell, J.A. 2014. Paleoenvironments during the Younger Dryas-Early  
 959 Holocene retreat of the Greenland Ice Sheet from outer Disko trough, central  
 960 west Greenland. *Journal of Quaternary Science*, 29, 27-40.
- 961 Jennings, A.E., Andrews, J.T., Pearce, C., Wilson, L., Ólfasdóttir, S. 2015. Detrital  
 962 carbonate peaks on the Labrador shelf, a 13-7 ka template for freshwater forcing  
 963 from the Hudson Strait outlet of the Laurentide Ice Sheet into the subpolar gyre.  
 964 *Quaternary Science Reviews*, 107, 62-80.
- 965 Jensen, J.F., Petersen, E.B., Olsen, B. 1999. „Sydostbugt Projekter“. New datings of  
 966 the Paleo-Eskimo Settlements in Qeqertarsuup Tunua (Disko Bugt), Greenland.  
 967 Copenhagen University, Archeological Notes p.2.
- 968 Jensen, J.F. 2006. Stone Age of Qeqertarsuup Tunua (Disko Bugt) a regional  
 969 analysis of the Saqqaq and Dorset cultures of Central West Greenland.  
 970 *Meddelelser om Grønland/Monographs on Greenland, Man & Society*, 32, 272 pp.  
 971 Danish Polar Centre.
- 972 Jensen, K.G., 2003. Holocene Hydrographic Changes in Greenland Coastal Waters.  
 973 Ph.D. thesis, The Geological Survey of Denmark and Greenland, Denmark.
- 974 Jiang, H., Siedenkrantz, M.-S., Knudsen, K.L., Eiríksson, J. 2001. Diatom surface  
 975 sediment assemblages around Iceland and their relationship to oceanic  
 976 environmental variables. *Marine Micropaleontology*, 41, 73-96.
- 977 Jiang, H., Seidenkrantz, M.S., Knudsen, K.L., Eiríksson, J. 2002. Late-Holocene  
 978 summer sea surface temperatures based on a diatom record from the north  
 979 Icelandic shelf. *The Holocene*, 12, 137-147.
- 980 Justwan, A., Koç, N. 2008. A diatom based transfer function for reconstructing sea  
 981 ice concentrations in the North Atlantic. *Marine Micropaleontology*, 66, 264-278.
- 982 Kaplan, M.R., Wolfe, A.P. 2006. Spatial and temporal variability of Holocene  
 983 temperature trends in the North Atlantic sector. *Quaternary Research*, 65, 223-  
 984 231.
- 985 Kaufman, D.S., et al. 2004. Holocene thermal maximum in the western Arctic

986 (0e180 degrees W). *Quaternary Science Reviews*, 23, 529-560.

987 Kelly, M. 1980. The status of the Neoglacial in western Greenland. *Rapport*  
988 *Grønlands Geologiske Undersøgelse*, 96, 1-24.

989 Kelley, S.E., Briner, J.P., Young, N.E. 2013. Rapid ice retreat in Disko Bugt  
990 supported by <sup>10</sup>Be dating of the last recession of the western Greenland Ice  
991 Sheet. *Quaternary Science Reviews*, 82, 13-22.

992 Knudsen, K. L., Søndergaard, M. K. B., Eiríksson, J., Jiang, H. 2008. Holocene  
993 thermal maximum off North Iceland: evidence from benthic and planktonic  
994 foraminifera in the 8600–5200 cal year BP time slice. *Marine Micropaleontology*,  
995 67, 120-142.

996 Korsun, S., Hald, M. 1998. Modern benthic foraminifera off Novaya Zemlya  
997 tidewater glaciers, Russian Arctic. *Arctic and Alpine Research*, 30, 61–77.

998 Koç Karpuz, N., Schrader, H. 1990. Surface sediment diatom distribution and  
999 Holocene paleotemperature variations in the Greenland, Iceland and Norwegian  
1000 Sea. *Paleoceanography*, 5, 557-580.

1001 Krawczyk, D., Witkowski, A., Moros, M., Lloyd, J.M., Kuijpers, A., Kierzek, A. 2010.  
1002 Late-Holocene diatom-inferred reconstruction of temperature variations of the  
1003 West Greenland Current from Disko Bugt, central West Greenland. *The Holocene*,  
1004 20, 659-666.

1005 Krawczyk, D., Witkowski, A., Wroniecki, M., Waniek, J., Kurzydłowski, K.J.,  
1006 Płociński, T. 2012. Reinterpretation of two diatom species from the West  
1007 Greenland margin - *Thalassiosira kushirensis* and *Thalassiosira antarctica* var.  
1008 *borealis* - hydrological consequences. *Marine Micropaleontology*, 88-89, 1-14.

1009 Krawczyk, D. W., Witkowski, A., Lloyd, J.M., Moros, M., Harff, J., Kuijpers, A. 2013.  
1010 Late-Holocene diatom derived seasonal variability in hydrological conditions off  
1011 Disko Bugt, West Greenland. *Quaternary Science Reviews*, 67, 93-104

1012 Krawczyk, D., Witkowski, A., Waniek, J., Wroniecki, M., Harff, J. 2015. Description of  
1013 diatoms from the southwest to west Greenland coastal and open marine waters.  
1014 *Polar Biology*, 538, 99-116. DOI: 10.1007/s00300-014-1546-2.

1015 Kuijpers, A., Mikkelsen, N., Ribeiro, S., Seidenkrantz, M.-S. 2014. Impact of  
1016 Medieval fjord hydrography and climate on the Western and Eastern settlements  
1017 in Norse Greenland. *Journal of the North Atlantic Special Volume*, 6, 1-13.

1018 Larsen, N. K., Kjær, K. H., Lecavalier, B., Bjørk, A. A., Colding, S., Huybrechts, P.,  
1019 Jakobsen, K.E Kjeldsen, K.K., Knudsen, K.-L., Odgaard, B.V., Olsen, J. (2015).  
1020 The response of the southern Greenland ice sheet to the Holocene thermal  
1021 maximum. *Geology*, G36476-1.

1022 Levac, E., de Vernal, A., Blake, W. Jr. 2001. Holocene paleoceanography of the  
1023 northernmost Baffin Bay: palynological evidence. *Journal of Quaternary Science*,  
1024 16, 353-363.

1025 Levinsen, H., Turner, J.T., Nielsen, T.G., Hansen, B.W. 2000. On the trophic  
1026 coupling between protists and copepods in arctic marine ecosystems. *Marine*  
1027 *Ecology Progress Series*, 204, 65-77.



1028 Lloyd, J.M., Park, L.A., Kuijpers, A., Moros, M. 2005. Early Holocene  
1029 palaeoceanography and deglacial chronology of Disko Bugt, West Greenland.  
1030 *Quaternary Science Reviews*, 24, 1741-1755.

1031 Lloyd, J.M. 2006. Modern distribution of benthic foraminifera from Disko Bugt, west  
1032 Greenland. *Journal of Foraminiferal Research*, 36, 315-331.

1033 Lloyd, J.M., Kuijpers, A., Long, A., Moros, M., Park, L.A. 2007. Foraminiferal  
1034 reconstruction of mid- to late-Holocene ocean circulation and climate variability in  
1035 Disko Bugt, West Greenland. *The Holocene*, 17, 1079-1091.

1036 Lloyd, J.M., Moros, M., Perner, K., Telford, R., Kuijpers, A., Jansen, E., McCarthy,  
1037 D.J. 2011. A 100 year record of ocean temperature control on the stability of  
1038 Jakobshavn Isbræ, West Greenland. *Geology*, 39, 867-870.

1039 Long, A.J., Roberts, D.H. 2003, Late Weichselian deglacial history of Disko Bugt,  
1040 West Greenland, and the dynamics of the Jakobshavns Isbræ ice stream.  
1041 *Boreas*, 32, 208-226.

1042 Matthews, J. 1969. The assessment of a method for the determination of absolute  
1043 pollen frequencies. *New Phytologist*, 68, 161–166.

1044 McGhee, R. 1996. Ancient People of the Arctic. UCB Press, Vancouver.

1045 McGovern, T., 1991. 'Climate Correlation and Causation in Norse Greenland. *Arctic*  
1046 *Anthropology*, 28, 77-100.

1047 Meldgaard, M., 2004. Ancient Harp Seal Hunters of Disko Bugt. Subsistence and  
1048 Settlement at the Saqqaq Culture Site Qeqertasussuk (2400 – 1400 BC), West  
1049 Greenland. *Meddelelser om Grønland/Monographs on Greenland, Man & Society*,  
1050 30, 1-189.

1051 Mertens, K.N. et al., 2009. Determining the absolute abundance of dinoflagellate  
1052 cysts in recent marine sediments: The *Lycopodium* marker-grain method put to  
1053 the test. *Review of Palaeobotany and Palynology*, 157, 238–252.

1054 Moon, T., Joughin, I. 2008. Changes in ice front position on Greenland's outlet  
1055 glaciers from 1992 to 2007. *Journal of Geophysical Research-Earth Surface*, 113  
1056 F02022, doi: 10.1029/2007JF000927.

1057 Moros, M., Kuijpers, A., Snowball, I., Lassen, S., Bäckström, D., Gingele, F.,  
1058 McManus, J. 2002. Were glacial iceberg surges in the North Atlantic triggered by  
1059 climatic warming? *Marine Geology*, 192, 393-417.

1060 Moros, M., Emeis, K., Risebrobakken, B., Snowball, I., Kuijpers, A., McManus, J.,  
1061 Jansen, E. 2004. Sea surface temperatures and ice rafting in the Holocene North  
1062 Atlantic: climate influences on northern Europe and Greenland. *Quaternary*  
1063 *Science Reviews*, 23, 2113-2126.

1064 Moros, M., Andrews, J.T., Eber, D.D., Jansen, E. 2006a. Holocene history of  
1065 drift ice in the northern North Atlantic: Evidence for different spatial and temporal  
1066 modes. *Paleoceanography*, 21, doi:10.1029/2005PA001214.

1067 Moros, M., Jensen, K.G., Kuijpers, A. 2006b. Mid- to late- Holocene hydrological and  
1068 climatic variability in Disko Bugt, central West Greenland. *The Holocene*, 16, 357–  
1069 367.

- 1070 Moros, M., Jansen, E., Oppo, D., Giraudeau, J., Kuijpers, A. 2012. Reconstruction of  
1071 the late Holocene changes in the Sub-Arctic Front position at the Reykjanes  
1072 Ridge, north Atlantic. *The Holocene*, 22, 877-886.
- 1073 Møller, H.S., Jensen, K.G., Kuijpers, A., Aagaard-Sørensen, S., Seidenkrantz, M.-S.,  
1074 Endler, R., Mikkelsen, N. 2006. Late Holocene environmental and climatic  
1075 changes in Ameralik Fjord, Southwest Greenland – evidence from the  
1076 sedimentary record. *The Holocene*, 16, 685-695.
- 1077 Mudie, P.J., Keen, C.E., Hardy, I.E., Vilks, G. 1984. Multivariate analysis and  
1078 quantitative paleoecology of benthic foraminifera in surface and Late Quaternary  
1079 shelf sediments, northern Canada. *Marine Micropalaeontology*, 8, 283–313.
- 1080 Murray, J.W. 1991. Ecology and palaeoecology of benthic foraminifera. Longman,  
1081 London, 397pp.
- 1082 Müller P.J., Kirst G., Ruhland G., von Storch I., and Rosell-Mele, B., 1998,  
1083 Calibration of the alkenone paleotemperature index UK37' based on core- tops  
1084 from the eastern southern South Atlantic and the global ocean (60°N-60°S):  
1085 *Geochimica Cosmochimica Acta* v. 62, p. 1757-1772.
- 1086 Müller, J., Werner, K., Stein, R., Fahl, K., Moros, M., Jansen, E. 2012. Holocene  
1087 cooling culminates in sea ice oscillations in Fram Strait. *Quaternary Science*  
1088 *Reviews*, 47, 1-14.
- 1089 Nielsen, N., Humlum, O., Hansen, B.U. 2001. Meteorological observations in 2000 at  
1090 the Arctic Station, Queqertarsuaq (69\_150N), Central West Greenland. *Danish*  
1091 *Journal of Geography*, 101, 155-157.
- 1092 Nørgaard-Pedersen, N. and Mikkelsen, N. 2009. 8000 year marine record of climate  
1093 variability and fjord dynamics from Southern Greenland. *Marine Geology*, 264,  
1094 177-189.
- 1095 Ólafsdóttir, S., Jennings, A. E., Geisdóttir, Á., Andrews, J., Miller, G. 2010.  
1096 Holocene variability of the North Atlantic Irminger current on the south- and  
1097 northwest shelf of Iceland. *Marine Micropaleontology*, 77, 101-118.
- 1098 Oppo, D.W., McManus, J.F., Cullen, J.L. 2003. Deepwater variability in the Holocene  
1099 epoch. *Nature*, 422, 277–278.
- 1100 Ouellet-Bernier M.-M. 2014. Changements paléocéanographiques dans la région de  
1101 Disko Bugt, Groenland, au cours de l'Holocène. Master thesis dissertation,  
1102 Université du Québec à Montréal.
- 1103 Ouellet-Bernier, M.-M., de Vernal, A., Hillaire-Marcel, C., Moros, M. 2014.  
1104 Paleoceanographic changes in the Disko Bugt area, West Greenland, during the  
1105 Holocene. *The Holocene*, 24, 1573-1583.
- 1106 Perner, K., Moros, M., Lloyd, J.M., Kuijpers, A., Telford, R.J., Harff, J. 2011.  
1107 Centennial scale benthic foraminiferal record of late Holocene oceanographic  
1108 variability in Disko Bugt, West Greenland. *Quaternary Science Reviews*, 30, 2815-  
1109 2826.
- 1110 Perner, K., Moros, M., Jennings, A., Lloyd, J.M., Knudsen, K.L. 2013a. Holocene  
1111 palaeoceanographic evolution off West Greenland. *The Holocene*, 23, 374-387
- 1112 Perner, K., Moros, M., Snowball, I., Lloyd, J.M., Kuijpers, A., Richter, T. 2013b.  
1113 Establishment of modern circulation pattern at c. 6000 cal a BP in Disko Bugt,

1114 central West Greenland: opening of the Vaigat Strait. *Journal of Quaternary*  
1115 *Science*, 28, 480-489.

1116 Polyak, L., Solheim, A. 1994. Late- and postglacial environments in the  
1117 northern Barents Sea west of Franz Josef Land. *Polar Research*, 13, 197–207.

1118 Polyakov, I., Bekryaev, R.V., Alekseev, G.V., Bhatt, U., Colony, R., Johnson, M.A.,  
1119 Walsh, D., and Makshtas, A.P. 2002. Variability and trends of air temperature and  
1120 pressure in the maritime Arctic, 1875–2000. *Journal of Climate*, 16, 2067–2077.

1121 Pritchard, H.D., Arthem, R.J., Vaughan, D.G., Edwards L.A. 2009. Extensive  
1122 dynamic thinning on the margins of the Greenland and Antarctic ice sheets.  
1123 *Nature*, 461, 971-975.

1124 Quillfeldt, C.H. 2001. Identification of some easily confused common diatom species  
1125 in Arctic spring blooms. *Botanica Marina*, 44, 375-389.

1126 Quillfeldt, C.H. 2004. The diatom *Fragilariopsis cylindrus* and its potential as an  
1127 indicator species for cold water rather than for sea ice. *Viet et Milieu*, 54, 137-143.

1128 Radi, T., et al. 2013. Operational taxonomy and (paleo-)autecology of round, brown,  
1129 spiny dinoflagellate cysts from the Quaternary of high northern latitudes. *Marine*  
1130 *Micropaleontology*, 98, 41–57.

1131 Ran, L., Jiang, H., Knudsen, K. L., Eiriksson, J., Gu, Z. 2006. Diatom response to the  
1132 Holocene climatic optimum on the North Icelandic shelf. *Marine*  
1133 *Micropaleontology*, 60, 226-241.

1134 Reimer, P.J., et al. 2009. IntCal09 and Marine09 radiocarbon age calibration curves,  
1135 0-50,000 years cal BP. *Radiocarbon*, 51, 1111-1150.

1136 Ribeiro, S., Moros, M., Ellegaard, M., Kuijpers, A. 2012. Climate variability in West  
1137 Greenland during the past 1500 years: evidence from a high-resolution marine  
1138 palynological record from Disko Bay. *Boreas*, 41, 68-83.

1139 Ribergaard, M.H., Kliem, N., Jespersen, M. 2006. HYCOM for the North Atlantic  
1140 Ocean with special emphasis on West Greenland Water. *Technical Report 06-0*.  
1141 [www.dmi.dk/dmi/tr06-07](http://www.dmi.dk/dmi/tr06-07).

1142 Ribergaard, M.H. 2013. Oceanographic Investigations off West Greenland 2012.  
1143 *NAFO Scientific Council Documents*, 13/003.

1144 Rignot, E., Kanagaratnam, P. 2006. Changes in the velocity structure of the  
1145 Greenland ice sheet. *Science*, 311, 986-990.

1146 Rignot, E., Koppes, M., Velicogna, I. 2010. Rapid submarine melting of the calving  
1147 faces of West Greenland glaciers. *Nature Geoscience*, 3, 187.

1148 Roberts, D.H., Long, A.J. 2005. Streamlined bedrock terrain and fast ice flow,  
1149 Jakobshavns Isbrae, West Greenland: implications for ice stream and ice sheet  
1150 dynamics. *Boreas*, 34, 25-42.

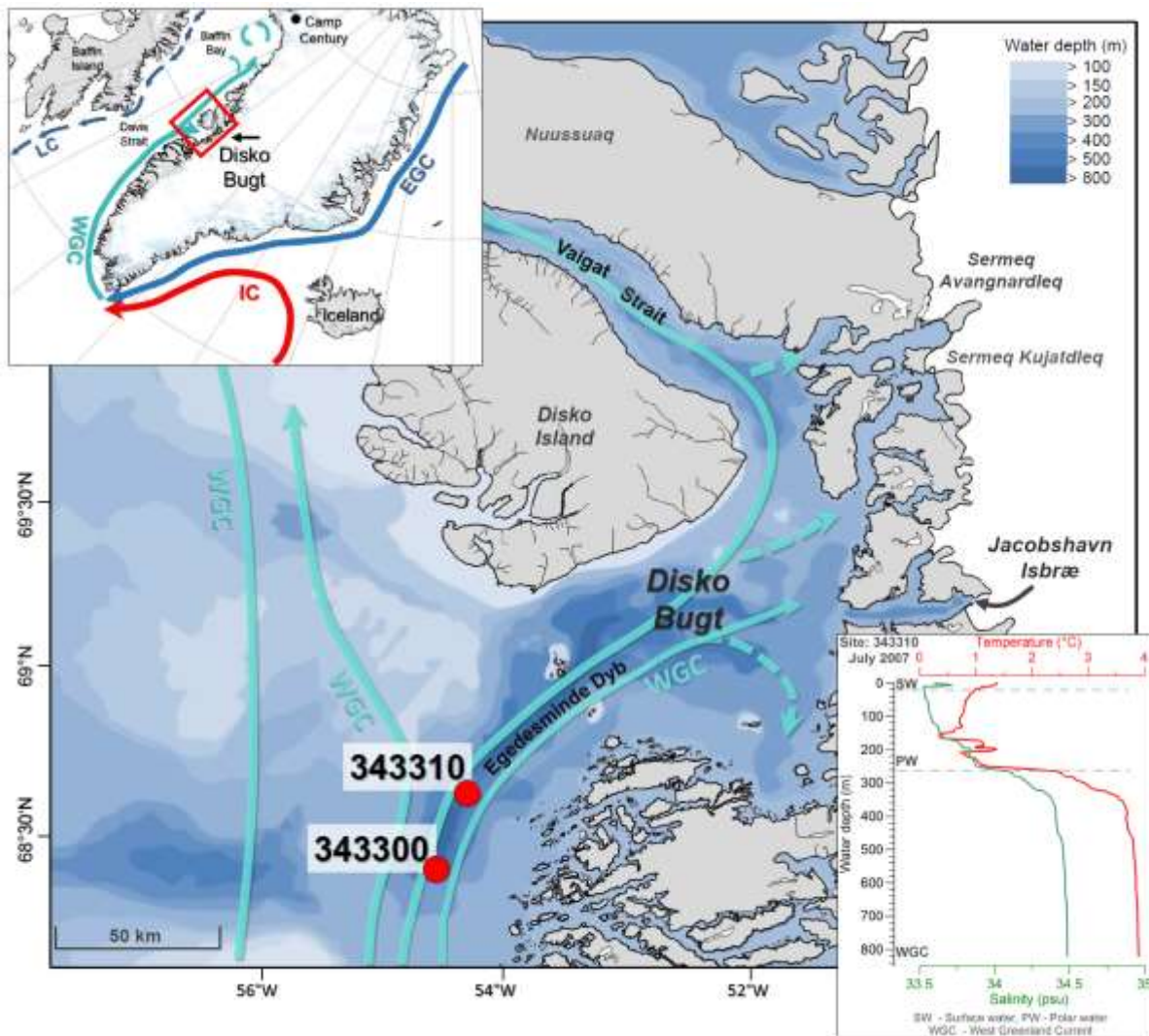
1151 Rochon, A., de Vernal, A., Turon, J.L., Matthiessen, J., Head, M.J. 1999. Distribution  
1152 of dinoflagellate cyst assemblages in surface sediments from the North Atlantic  
1153 Ocean and adjacent basins and quantitative reconstruction of sea-surface  
1154 parameters, Special Contribution Series, American Association of Stratigraphic  
1155 Palynologists, n° 35.

- 1156 Rosell-Melé, A. 1998. Interhemispheric appraisal of the value of alkenone indices as  
1157 temperature and salinity proxies in high latitude locations. *Paleoceanography*, 13,  
1158 694.
- 1159 Rosell-Melé, A., Jansen, E., Weinelt, M. 2002. Appraisal of a molecular approach to  
1160 infer variations in surface ocean freshwater inputs into the North Atlantic during  
1161 the last glacial. *Global and Planetary Change*, 34, 143-152.
- 1162 Rytter, F., Knudsen, K.L., Seidenkrantz, S., Eiriksson, J. 2002. Modern  
1163 distribution of benthic foraminifera on the North Icelandic shelf and slope. *Journal*  
1164 *of Foraminiferal Research*, 32, 217–244.
- 1165 Schafer, C.T, Cole, F.E. 1986. Reconnaissance survey of benthonic foraminifera  
1166 Schrader, H.J., Gersonde, R. 1978. Diatoms and Silicoflagellates. In: Zachariasse et  
1167 al. (Eds.), *Micropaleontological counting methods and techniques and exercise on*  
1168 *an eight meters section of the lower Pliocene of Capo Rosello, Silicy. Utrecht*  
1169 *Micropaleontological Bulletins* 17, 129-176.  
1170 from Baffin Fjord environments. *Arctic*, 39, 232–239.
- 1171 Seidenkrantz, M.-S., Roncaglia, L., Fischel, A., Heilmann-Clausen, C., Kuijpers,  
1172 A., Moros, M. 2008. Variable North Atlantic seesaw patterns documented by a late  
1173 Holocene marine record from Disko Bugt, West Greenland. *Marine*  
1174 *Micropaleontology*, 68, 66-83.
- 1175 Seidenkrantz, M.-S., Ebbesen, H., Aagaard-Sørensen, S., Moros, M., Lloyd, J.,  
1176 Olsen, J., Knudsen, M.F., Kuijpers, A. 2013. Early Holocene large-scale meltwater  
1177 discharge from Greenland documented by foraminifera and sediment parameters.  
1178 *Palaeogeography, Palaeoclimatology, Palaeoecology* 391, 71-81.
- 1179 Sejrup, H.P., Birks, H.J.B., Klitgaard-Kristensen, D., Madsen, H. 2004. Benthonic  
1180 foraminiferal distributions and quantitative transfer functions for the northwest  
1181 European continental margin. *Marine Micropaleontology*, 53, 197-226.
- 1182 Sicre, M. A., Bard, E., Ezat, U., Rostek, F. 2002. Alkenone distributions in the North  
1183 Atlantic and Nordic sea surface waters. *Geochem. Geophys. Geosyst.*, 3, 1013,  
1184 doi:10.1029/2001GC00015
- 1185 Steinsund, P.I., Polyak, L., Hald, M., Mikhailov, V., Korsun, S. 1994. Distribution of  
1186 calcareous benthic foraminifera in recent sediments of the Barents and Kara Sea.  
1187 In: Steinsund, P.I., *Benthic foraminifera in surface sediments of the Barents and*  
1188 *Kara Seas: modern and late Quaternary application*. Ph.D. thesis, Department of  
1189 *Geology, Institute of Biology and Geology, Univeristy of Tromsø*.
- 1190 Straneo, F., Hamilton, G.S., Sutherland, D.A., Stearns, L.A., Davidson, F., Hammill,  
1191 M.O., Stenson, G.B., Rosing-Asvid, A. 2010. Rapid circulation of subtropical  
1192 waters in a major fjord in East Greenland. *Nature Geoscience*, 3, 182-186.
- 1193 Syvertsen, E.E. 1979. Resting spore formation in clonal cultures of *Thalassiosira*  
1194 *antarctica* Comber, T. *nordenskioldii* Cleve and *Detonula confervacea* (Cleve)  
1195 *Gran. Nova Hedwigia*, 64, 4-63.
- 1196 Tang, C.C.L., Ross, C.K., Yao, T., Petrie, B., De Tracey, B.M., Dunlap, E. 2004. The  
1197 circulation, water mass and sea-ice of Baffin Bay. *Progress in Oceanography*, 63,  
1198 183-228.

- 1199 Takano, H., 1985. Two new diatoms in the genus *Thalassiosira* from Japanese  
1200 marine waters. *Tokai Regional Fisheries Research Laboratory*, 116, 1-9.
- 1201 Telesinski, M.M., Spielhagen, R.F., Bauch, H.A. 2014. Water mass evolution of the  
1202 Greenland Sea since late glacial times. *Climate of the Past*, 10, 123-136.
- 1203 Thornalley, D.J.R., Elderfield, H., McCave, I.N. 2009. Holocene oscillations in  
1204 temperature and salinity of the surface subpolar North Atlantic. *Nature*, 457, 711–  
1205 714
- 1206 Throndsen, J., Hasle, G.R., Tangen, K. 2003. Norsk Krystplanktonflora. *Almater*  
1207 *Forlag As*, Oslo, Norway.
- 1208 Vilks, G. 1981. Late glacial–postglacial foraminiferal boundary in sediments of  
1209 eastern Canada, Denmark and Norway. *Geoscience Canadian*, 8, 48–56.
- 1210 Vinther, B. M., et al., 2009. Holocene thinning of the Greenland ice sheet. *Nature*,  
1211 461, 385-388.
- 1212 Walsh, K.M., Howat, I.M., Ahn, Y., Enderlin, E.M. 2012. Changes in the marine-  
1213 terminating glaciers of central east Greenland, 2000-2010. *The Cryosphere*, 6,  
1214 211-220.
- 1215 Wanner, H., Solomina, O., Grosjean, M., Ritz, S. P., Jetel, M. 2011. Structure and  
1216 origin of Holocene cold events. *Quaternary Science Reviews*, 30, 3109-3123.
- 1217 Weckström, K., Miettinen, A., Caissie, B., Pearce, C., Ellegaard, M., Krawczyk, D.,  
1218 Witkowski, A. 2014. Sea surface temperatures in Disko Bay during the Little Ice  
1219 Age – caution needs to be exercised before assigning *Thalassiosira kushirensis*  
1220 resting spore as a warm-water indicator in palaeoceanographic studies.  
1221 *Quaternary Science Reviews*, 101, 234-237.
- 1222 Weidick, A., Oerter, H., Reeh, N., Thomsen, H.H., Thorning, L. 1990. The  
1223 recession of the Inland Ice margin during the Holocene climatic optimum in the  
1224 Jakobshavn Isfjord area of West Greenland. *Palaeogeography,*  
1225 *Palaeoclimatology, Palaeoecology*, 82, 389–399.
- 1226 Weidick, A., Bennike, O. 2007 Quaternary glaciations history and glaciology of  
1227 Jakobshavn Isbræ and the Disko Bugt region, West Greenland: a review.  
1228 *Geological Survey of Denmark and Greenland Bulletin*, 14, 78pp.
- 1229 Williamson, M.A., Keen, C.E., Mudie, P.J. 1984. Foraminiferal distribution on  
1230 the continental margin off Nova Scotia. *Marine Micropaleontology*, 9, 219–239.
- 1231 Witkowski, A., Lange-Bertalot, H., Metzeltin, D. 2000. Diatom Flora of Marine  
1232 Coasts. In: *Iconographia Diatomologica 7*, Koeltz Scientific Books, Königstein,  
1233 Germany.
- 1234 Young, N.E., Briner, J.P. 2015. Holocene evolution of the western Greenland Ice  
1235 Sheet: Assessing geophysical ice-sheet models with geological reconstructions of  
1236 ice-margin change. *Quaternary Science Reviews* 114, 1 – 17.
- 1237 Young, N.E., Briner, J.P., Stewart, H.A.M., Axford, Y., Csatho, B., Rood, D.H.,  
1238 Rinkel, R.C. 2011 Response of Jakobshavn Isbræ, Greenland, to Holocene  
1239 climate change. *Geology*, 39, 131-134.
- 1240 Young, N.E., Schaefer, J.M., Briner, J.P., Goehring, B.M. 2013a. A Be-10 production  
1241 rate calibration for the Arctic. *Journal of Quaternary Science*, 28, 515-526.

- 1242 Young, N.E., Briner, J.P., Rood, D.H., Finkel, R.C., Corbett, L.B., Bierman, P.R.,  
1243 2013b. Age of the Fjord Stade moraines in the Disko Bugt region, western  
1244 Greenland, and the 9.3 and 8.2 ka cooling events. *Quaternary Science Reviews*,  
1245 60, 76-90.
- 1246 Zarudzki, E.F.K. 1980. Interpretation of shallow seismic profiles over the continental  
1247 shelf in West Greenland between latitudes 64° and 69° 30' N. *Geological Survey*  
1248 *of Greenland Report*, 100, 58-61.
- 1249 Zwally, H.J., Abdalati, W., Herring, T., Larson, K., Saba, J., Steffen, K. 2002,  
1250 Surface melt-induced acceleration of Greenland Ice-Sheet flow. *Science*, 297,  
1251 218-222.
- 1252

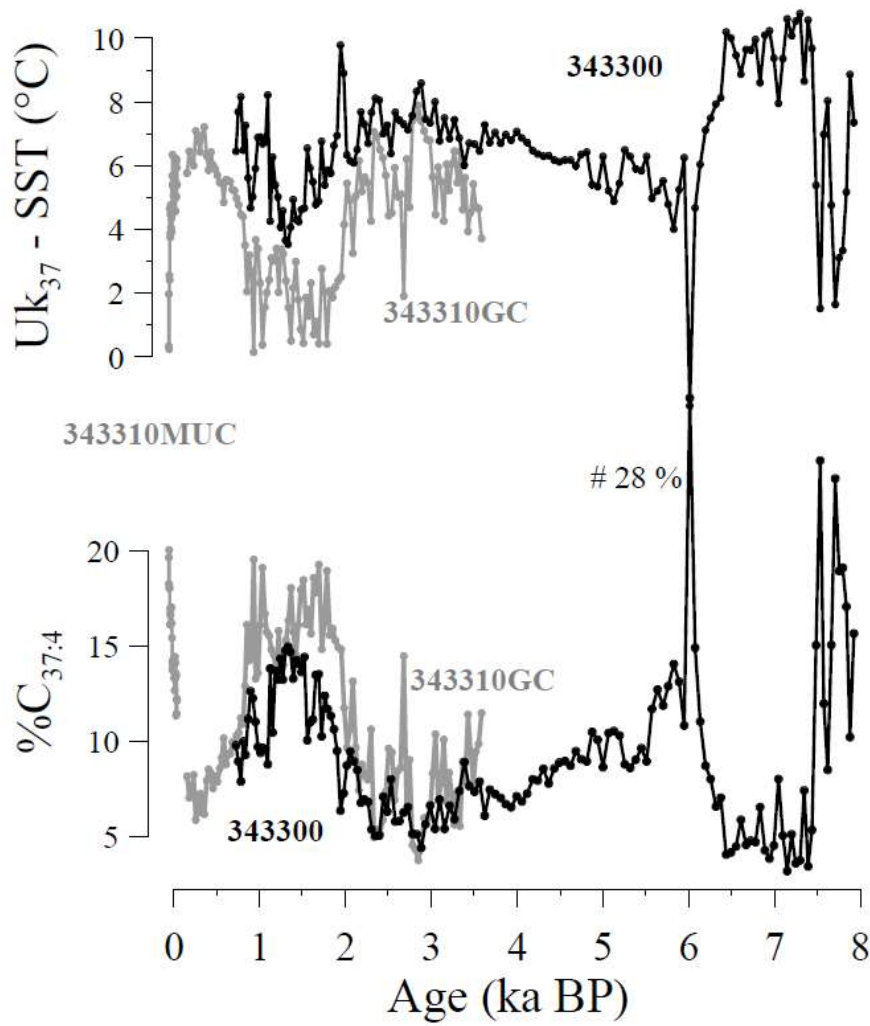
1253



1254

1255 Figure 1: Bathymetric map of Disko Bugt, adapted from Jakobsson et al. (2008) and  
1256 the present day oceanographic setting of the study area. The location of core  
1257 343300 at the southwest edge of Egedesminde Trough and of core 343310 in the  
1258 main Egedesminde Trough, are shown by red dots. The upper left inset shows the  
1259 oceanographic setting around Greenland. Abbreviations are as follows: EGC - East  
1260 Greenland Current; IC – Irminger Current; WGC – West Greenland Current; LC –  
1261 Labrador Current. Lower right inset: CTD profile at site 343310 from July 2007 the  
1262 year of sampling.

1263

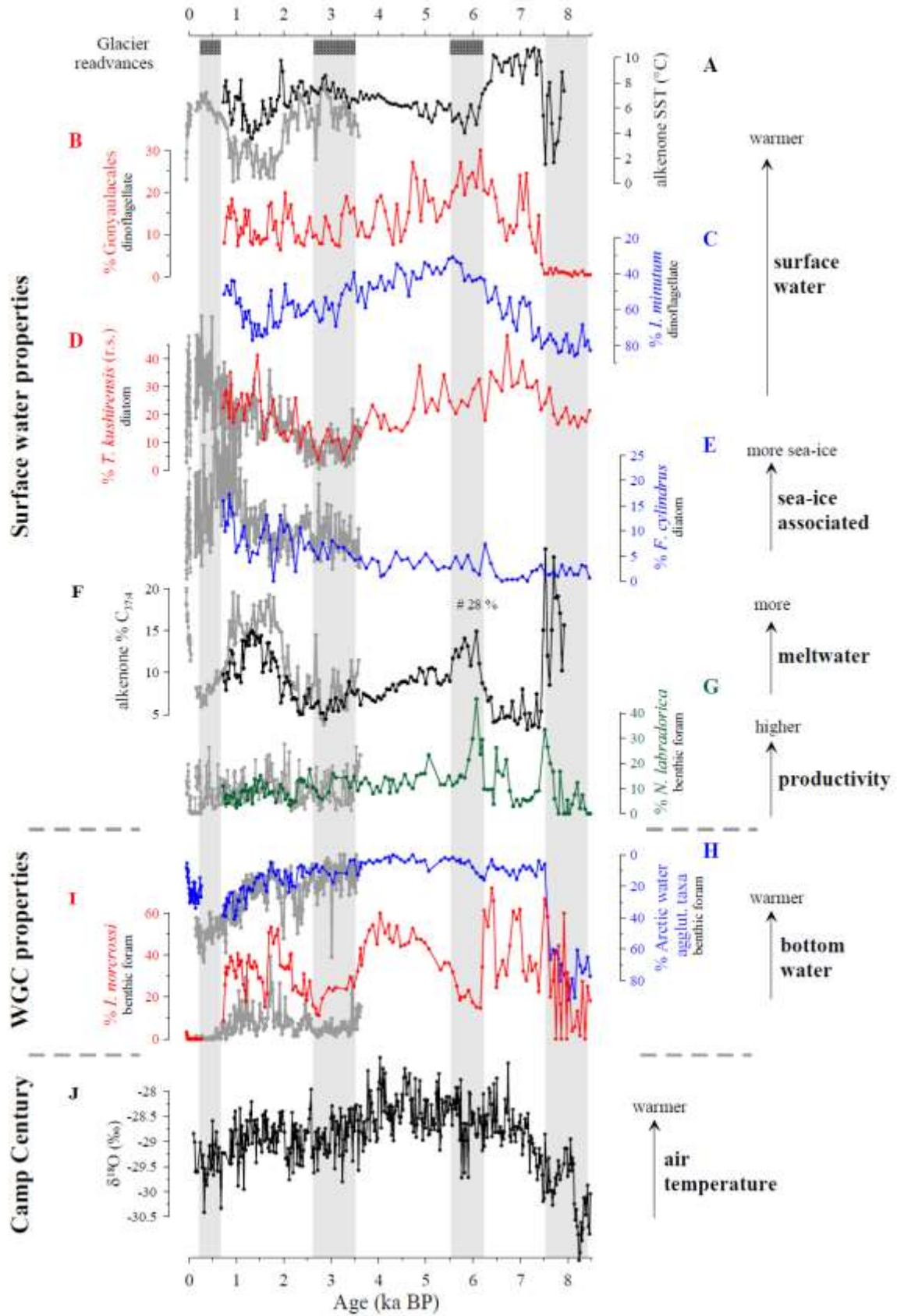


1265

1266 Figure 2. Holocene alkenone derived records of relative sea surface temperature  
 1267 ( $U^k_{37}$  index) and salinity variations ( $\%C_{37:4}$ ) from the core sites 343300 and 343310 in  
 1268 Egedeminde Trough. The dark line is from core 343300 and the grey line is from  
 1269 core 343310.

1270

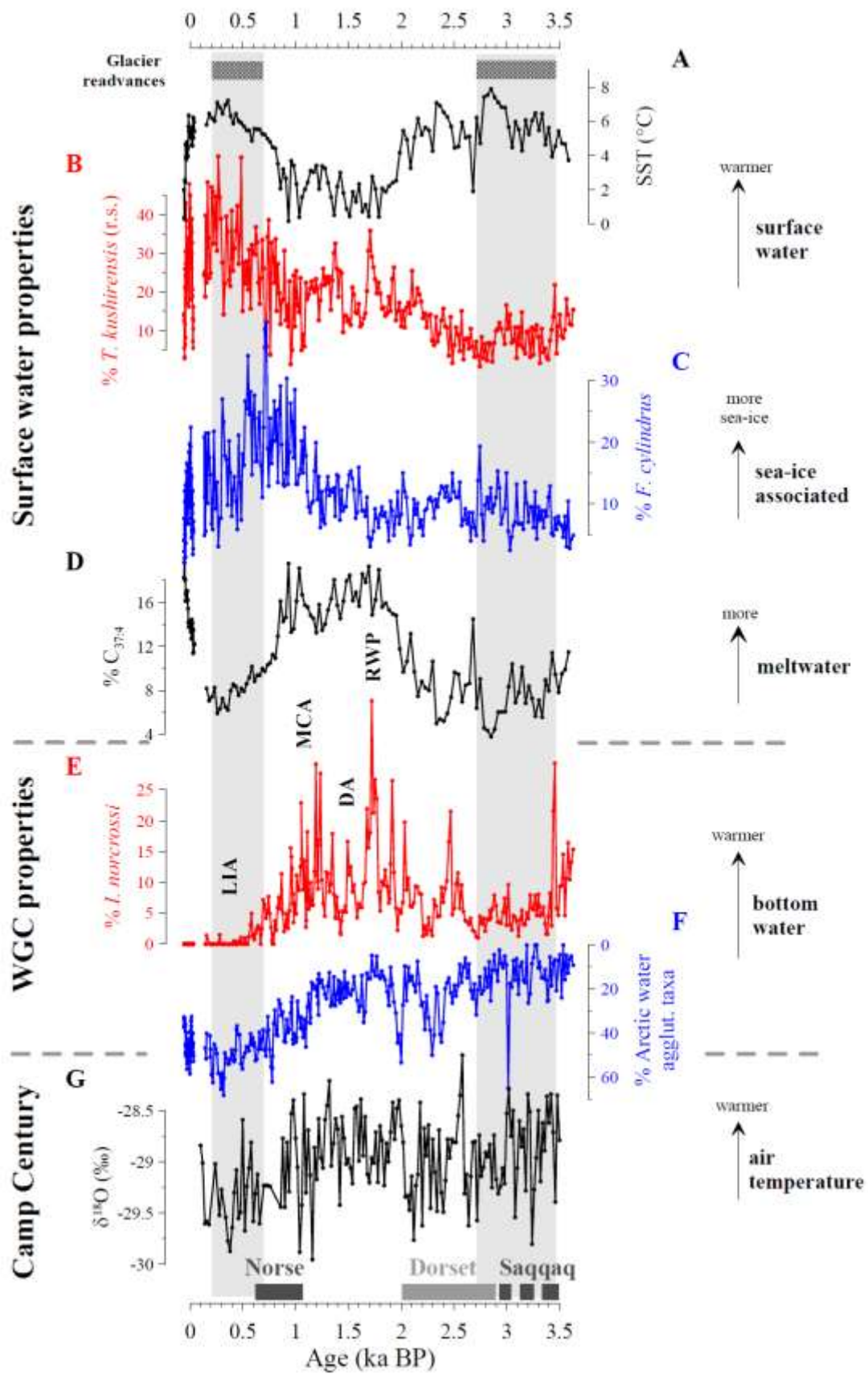




1271

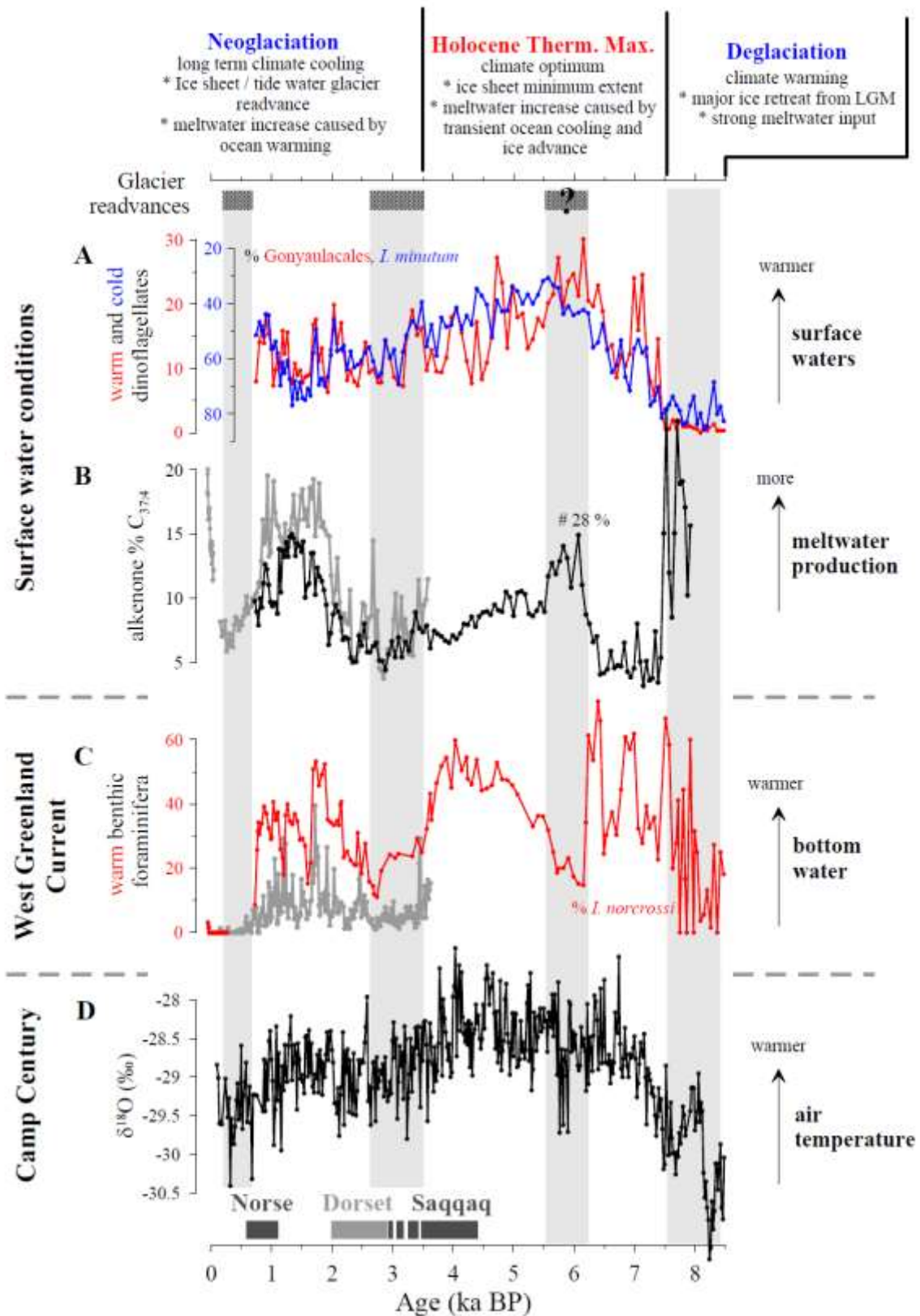
1272 Figure 3

1273



1274

1275 Figure 4.



1276

1277 Figure 5.

1278 Figure 3: Holocene palaeoenvironmental changes within the Disko Bugt area (longer  
1279 time series shown in dark shade are from core 343300, shorter time series shown in  
1280 grey shade are from core 343310). Surface water reconstructions (A – G): A)  
1281 Alkenone derived  $U_{37}^k$  index; B) Relative abundance (%) of dinoflagellate cysts of *P.*  
1282 *dalei*, a warm end member species; C) Relative abundance (%) of dinoflagellate *I.*  
1283 *minutum*, a cold end member taxa (note inverted scale); D) Relative abundance (%)  
1284 of diatom *T. kushirensis* r.s., the warmer water end member species; E) Relative  
1285 abundance of diatom *F. cylindrus* – the colder water end member species associated  
1286 with sea ice; F) the biomarker  $\%C_{37:4}$  – reflecting salinity variability; G) Relative  
1287 abundance (%) of the benthic foraminifer *N. labradorica* – indicating surface water  
1288 productivity variability. West Greenland Current properties (bottom water proxies) (H  
1289 – I): H) Relative abundance (%) of Arctic water agglutinated taxa – the cold water  
1290 end-member of the benthic foraminiferal assemblage (note inverted scale); I)  
1291 Relative abundance (%) of benthic foraminifera *I. norcrossi* - the warm water end-  
1292 member and; J)  $\delta^{18}O$  record of the Camp Century ice core shows variations of  
1293 atmospheric temperature from West Greenland. Vertical grey shaded bars mark  
1294 interpreted cold periods during the last ~8.3 ka BP. Dark grey horizontal bars at the  
1295 top of the diagram indicate Greenland glacier advances.

1296

1297 Figure 4: Late Holocene palaeoenvironmental changes from core 343310. Surface  
1298 water reconstructions (A – D): A) Alkenone derived  $U_{37}^k$  index records; B) Relative  
1299 abundance (%) of warmer water diatom species *T. kushirensis* r.s.; C) Relative  
1300 abundance (%) of the colder water, sea-ice associated diatom species *F. cylindrus*;  
1301 D) Relative abundance of  $\%C_{37:4}$  – reflecting salinity variability. West Greenland  
1302 Current properties (bottom water proxies) (E – F): E) Relative abundance (%) of *I.*  
1303 *norcrossi*, warm water benthic foraminiferal end member and; F) relative abundance  
1304 (%) of Arctic water benthic foraminiferal agglutinated taxa (note inverted scale); G)  
1305  $\delta^{18}O$  record of the Camp Century ice core showing variations of atmospheric  
1306 temperature from West Greenland. Vertical grey shaded bars mark interpreted cold  
1307 periods during the last ~3.5 ka BP. Dark grey horizontal bars at the top of the  
1308 diagram indicate Greenland glacier advances, shaded bars at the base of the  
1309 diagram indicate periods of Palaeo-Eskimo and Norse settlements in West  
1310 Greenland. Timing of known climate fluctuations: RWP - Roman Warm Period, DA –  
1311 Dark Ages, MCA – Medieval Climate Anomaly, LIA – Little Ice Age.

1312

1313 Figure 5. Summary of palaeoenvironmental interpretation: Upper panel) General  
1314 interpretation of the records split into the Deglaciation, Holocene Thermal Maximum  
1315 and Neoglaciation. Surface water conditions based on A) dinoflagellate warm (red)  
1316 and cold (blue) water taxa in core 343300 and on B)  $\%C_{37:4}$  from core 343300 (black  
1317 shade) and core 343310 (grey shade); C) West Greenland Current properties based  
1318 on  $\% I. norcrossi$  warm end member benthic foraminiferas species from core 343300  
1319 (red shade) and core 343310 (grey shade); D)  $\delta^{18}O$  record of the Camp Century ice  
1320 core showing variations of atmospheric temperature from West Greenland. Vertical

1321 grey shaded bars mark interpreted cold periods during the last ~3.5 ka BP. Dark grey  
1322 horizontal bars at the top of the diagram indicate Greenland glacier advances,  
1323 shaded bars at the base of the diagram indicate periods of Palaeo-Eskimo and  
1324 Norse settlements in West Greenland. Timing of known climate fluctuations: RWP -  
1325 Roman Warm Period, DA – Dark Ages, MCA – Medieval Climate Anomaly, LIA –  
1326 Little Ice Age.

1327

1328

1329